TABLE 1

Kinetic parameters of the uptake of H_2-receptor antagonists by organic anion transporter 3

K_m and V_{max} were determined by nonlinear regression analysis as described under *Materials and Methods*. Data are taken from Fig. 2. Each value represents the mean ± computer-calculated S.D. The value in parentheses represents the relative transport activity with regard to cimetidine transport.

Isoform	Cimetidine			Famotidine			Ranitidine		
	K_m	V_{max}	V_{max}/K_m	K_m	V_{max}	V_{max}/K_m	K_m	V_{max}	V_{max}/K_m
	μM	*pmol/min/mg protein*	*μl/min/mg protein*	*μM*	*pmol/min/mg protein*	*μl/min/mg protein*	*μM*	*pmol/min/mg protein*	*μl/min/mg protein*
mkOAT3	70.9 ± 4.1	274 ± 9	3.86 (1)	154 ± 14	190 ± 11	1.23 (0.32)	125 ± 14	154 ± 12	1.27 (0.33)
hOAT3[a]	149 ± 35	1470 ± 230	9.86 (1)	124 ± 4	448 ± 10	3.61 (0.37)	234 ± 49	551 ± 49	2.35 (0.24)
rOat3[a]	90.7 ± 4.8	512 ± 17	5.64 (1)	345 ± 22	252 ± 12	0.73 (0.13)	155 ± 9	1660 ± 63	10.7 (1.90)

[a] Tahata et al., 2005a.

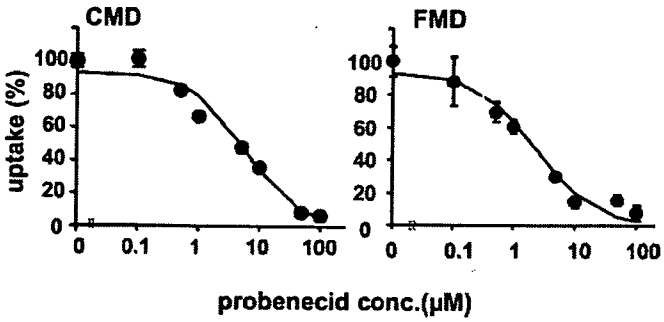

Fig. 3. Inhibitory effect of probenecid on the uptake of cimetidine and famotidine by mkOAT3-HEK. The uptake of CMD and FMD (10 μM) by mkOAT3 for 3 min was determined in the absence or presence of probenecid at the designated concentrations. The values were expressed as a percentage of cimetidine or famotidine transport by mkOAT3-HEK in the presence of probenecid versus that in the absence of probenecid. The rigid line represents the fitted line obtained by nonlinear regression analysis as described under *Materials and Methods*. Each point represents the mean ± S.E. (n = 3).

nonrenal clearance of famotidine was reduced from 0.445 ± 0.168 to 0.244 ± 0.029 l/h/kg, although this was not statistically significant ($p > 0.05$).

Effect of Probenecid on the Pharmacokinetics of Cimetidine in the Monkeys. The mean plasma concentration time profiles of cimetidine in the cynomolgus monkey are shown in Fig. 4B. The mean plasma pharmacokinetic parameters are summarized in Table 3. The urinary recovery over the 0- to 24-h collection period and the renal and tubular secretion clearances are included in Table 3. As observed in Fig. 4B and Table 3, probenecid had very little effect on the pharmacokinetics of cimetidine in the cynomolgus monkeys. Probenecid treatment produced no significant difference in any of the pharmacokinetic parameters of cimetidine. The fp and fe in cynomolgus monkeys with or without probenecid treatment were determined as 79.1 ± 4.8 versus 81.7 ± 2.0% and 37.0 ± 3.9 versus 36.3 ± 3.9%.

Plasma Concentration of Probenecid in the Monkey. The mean plasma concentration time profiles of probenecid in cynomolgus monkeys are shown in Fig. 4C. The maximum (at 1 h) and minimum (at 8 h) plasma concentrations of probenecid were 76.8 ± 10.1 μg/ml (269 μM) and 23.3 ± 2.9 μg/ml (81.8 μM), respectively. Taking the unbound fraction in the plasma (13.1 ± 0.3%) into consideration, the maximum unbound concentration of probenecid (35 μM) in the monkey study was comparable with that observed in the human study (ca. 46 μM) (Inotsume et al., 1990).

Prediction of Renal Clearance of Famotidine by Allometric Scaling. The renal clearance and renal tubular secretion clearance of famotidine in rats (Lin et al., 1987),

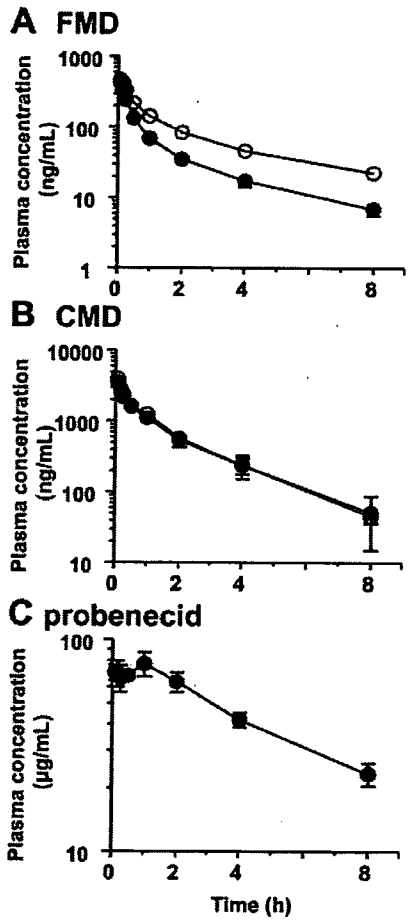

Fig. 4. Plasma concentrations of famotidine, cimetidine, and probenecid in the cynomolgus monkeys. Plasma concentrations of famotidine (A), cimetidine (B), and probenecid (C) in the cynomolgus monkeys after i.v. administration of famotidine and cimetidine at a dose of 0.3 and 4 mg/kg, respectively, following pretreatment with 22.5 mg/kg probenecid (open circles) or control (closed circles). Each data point was connected with the rigid line and represents the mean ± S.E. (n = 4).

dogs (Boom et al., 1997), and monkeys were analyzed as a function of species body weight (W) using the simple allometric equation for interspecies scaling and used to predict these parameters in humans. The corresponding allometric equations based on three species data were $CL_{renal} = 0.957 \times W^{0.710}$ and $CL_{sec} = 0.609 \times W^{0.679}$, respectively. The predicted values of CL_{renal} and CL_{sec} based on a 70-kg body weight in humans were 19.5 and 10.9 l/h, respectively, which were very similar to the observed values (13.3–18.2 and 8.31–13.2 l/h) (Inotsume et al., 1990; Gladziwa and Klotz, 1993).

TABLE 2

Pharmacokinetic parameters of famotidine in the cynomolgus monkeys

Pharmacokinetic parameters were determined by two-compartment model with nonlinear regression analysis as described under *Materials and Methods*. Each value represents the mean ± S.D. (n = 4). Data are taken from Fig. 4.

Probenecid	$t_{1/2\alpha}$	$t_{1/2\beta}$	$AUC_{0-\infty}$	CL_p	CL_{dis}	V_c	$V_{d,ss}$	CL_{renal}	CL_{sec}	$CL_{non\ renal}$
	h		*ng·h/ml*	*l/h/kg*		*l/kg*			*l/h/kg*	
Without	0.234 ± 0.058	2.69 ± 0.38	350 ± 48	0.870 ± 0.120	0.816 ± 0.116	0.573 ± 0.062	2.08 ± 0.28	0.426 ± 0.079	0.275 ± 0.075	0.445 ± 0.168
With	0.314 ± 0.087	3.58 ± 0.87	740 ± 80**	0.409 ± 0.044**	0.641 ± 0.100*	0.626 ± 0.141	1.60 ± 0.25*	0.165 ± 0.027**	0.0230 ± 0.0217*	0.244 ± 0.029
Ratio to control	1.4 (0.98–2.0)	1.3 (1.1–1.8)	2.1 (1.9–2.4)	0.47 (0.42–0.53)	0.79 (0.68–0.95)	0.96 (0.76–1.3)	0.77 (0.69–0.91)	0.36 (0.30–0.51)	0.078 (0.031–0.14)	0.61 (0.41–0.88)

Statistical differences were calculated between the probenecid-treated and untreated groups by two-tailed paired Student's t test with $p < 0.05$ as limit of significance (*, $p < 0.05$; **, $p < 0.01$).

TABLE 3

Pharmacokinetic parameters of cimetidine in the cynomolgus monkeys

Pharmacokinetic parameters were determined by two-compartment model with nonlinear regression analysis as described under *Materials and Methods*. Each value represents the mean ± S.D. (n = 4). Data are taken from Fig. 4. Statistical differences were calculated between the probenecid-treated and untreated groups by two-tailed paired Student's t test with $p < 0.05$ as limit of significance (*, $p < 0.05$; **, $p < 0.01$).

Probenecid	$t_{1/2\alpha}$	$t_{1/2\beta}$	$AUC_{0-\infty}$	CL_p	CL_{dis}	V_c	$V_{d,ss}$	CL_{renal}	CL_{sec}	$CL_{nonrenal}$
	h		*ng·h/ml*	*l/h/kg*		*l/kg*			*l/h/kg*	
Without	0.257 ± 0.122	1.70 ± 0.32	3970 ± 708	1.03 ± 0.17	1.27 ± 0.74	1.03 ± 0.19	1.97 ± 0.13	0.385 ± 0.061	0.222 ± 0.028	0.647±0.185
With	0.261 ± 0.117	1.64 ± 0.10	4140 ± 507	0.978 ± 0.123	1.13 ± 0.62	0.983 ± 0.187	1.82 ± 0.09	0.354 ± 0.066	0.216 ± 0.054	0.624 ± 0.148
Ratio to control	1.1 (0.80–1.8)	0.99 (0.75–1.2)	1.1 (0.99–1.1)	0.95 (0.91–1.0)	1.0 (0.49–1.6)	0.97 (0.78–1.2)	0.93 (0.79–1.0)	0.91 (0.84–1.0)	0.92 (0.86–1.0)	0.98 (0.82–1.2)

Discussion

In the present study, we examined whether the drug-drug interaction between famotidine and probenecid could be reproduced in monkeys. The transport activities of the H_2 receptor antagonists by mkOAT3 were compared with those by hOAT3, and the mRNA expression of the hOCT isoforms in the monkey kidney was quantified. To draw a definite conclusion, the effect of probenecid on the renal clearance of famotidine and cimetidine was examined in cynomolgus monkeys.

Famotidine was transported only by mkOAT3, whereas cimetidine and ranitidine are substrates of mkOAT1 and mkOAT3 (Fig. 1). The K_m values for mkOAT3-mediated uptake were similar to those for hOAT3 (Table 1). Previously, it had been shown that the uptake of cimetidine relative to the uptake of benzylpenicillin was similar for mk- and hOAT3 (Tahara et al., 2005b). This also holds true for famotidine uptake. In addition, the relative activity of famotidine exhibited by mkOAT3 was greater than that by rOat3, consistent with previous results in humans (Tahara et al., 2005a). These results support the hypothesis that the transport of the H_2 receptor antagonists by mkOAT3 is similar to that by hOAT3, rather than the rodent isoforms (Table 1).

OCT1 is the liver-specific isoform in humans, whereas it is expressed both in rodent liver and kidney (Motohashi et al., 2002; Slitt et al., 2002). This makes the contribution of organic cation transporters to renal uptake greater in rodents than in humans. Quantification of mRNA expression revealed that mkOCT1 and mkOCT2 are predominantly expressed in the liver and kidney, respectively, whereas mkOCT3 is expressed at considerably lower levels in these tissues. This expression patterns are similar to those in humans (Motohashi et al., 2002). Consequently, like human kidney, putative mkOCT2 plays a predominant role in the monkey kidney.

These results suggest that, as far as basolateral transporters are concerned, the monkey OATs and OCTs have similar characteristics to the human orthologs, and this prompted us to perform an in vivo study to obtain conclusive evidence. In monkeys, both famotidine and cimetidine are predominantly excreted into the urine, and the tubular secretion and glomerular filtrate rates that account for their renal clearance, are almost identical (Tables 2 and 3). When probenecid was given orally, the renal and renal tubular secretion clearance were reduced by 65 and 90%, respectively, resulting in a 2.0-fold increase in the AUC (Fig. 4A; Table 2). In addition, the steady-state distribution volume was reduced by 23% by probenecid. This is consistent with the previous findings in humans (Inotsume et al., 1990). It seems that the inhibition of the uptake by tissues, including the kidney, accounts for this effect. On the other hand, the plasma concentration and renal clearance or distribution clearance of cimetidine were not affected by probenecid (Fig. 4B; Table 3). Probenecid achieves a clinically relevant unbound concentration in monkey plasma (11–35 μM), which is sufficient to markedly inhibit mkOAT3, suggesting that the interaction could involve mkOAT3-mediated uptake, at least in part. Taking into account the degree of inhibition of tubular secretion clearance by probenecid, the probenecid-sensitive transporter, mkOAT3, plays a major role in the renal tubular secretion of famotidine, but not cimetidine, in monkeys. These results are consistent with the clinical studies (Gisclon et al., 1989; Inotsume et al., 1990). Consequently, monkeys, rather than rodents, can be used to predict drug-drug interactions involving tubular secretion, particularly when multiple transporters are involved.

The nonrenal clearance of famotidine was smaller in monkeys treated with probenecid than in the control group (Table 2). Although the difference was not statistically significant, it is likely that increasing the number of animals will make this difference statically significant. The presence of the oxidized metabolite of famotidine in human urine suggests that famotidine undergoes hepatic metabolism (Kroemer and Klotz, 1987). Because probenecid had no effect on OCT1, a candidate transporter responsible for the hepatic uptake of famotidine (Tahara eta al., 2005a), the reduction in the nonrenal clearance of famotidine by probenecid may be caused by inhibition of this metabolism. Currently, there is no report showing that probenecid has an inhibitory effect on metabolism, and this should be examined in future studies.

Interspecies scaling has been successfully used to predict human pharmacokinetic parameters from animals based on the concept of allometry (Lin, 1995; Reigner et al., 1997). It has been shown that simple allometric scaling of the renal clearance is a good predictor for drugs, such as methotrexate and several β-lactam antibiotics (Dedrick et al., 1970; Matsushita et al., 1990), although this is not the case for betamipron and enprofylline (Mahmood, 1998). The renal and renal tubular secretion clearances of famotidine in humans were estimated by simple allometric scaling using data from rats, dogs, and monkeys. A good predictability of the absolute values of the renal and renal tubular clearances from animal experiments (rat, dog and monkey) was observed, although the contribution of the renal transporters differs depending on the species. Therefore, good predictability by the allometric scaling cannot exclude the possibility of a species-dependent contribution by basolateral transporters. In particular, for the quantitative prediction of drug-drug interactions in humans, the contribution of transporters should be estimated using human materials. Alternatively, the relative activity factor method can be applied to predict the in vivo contribution of basolateral organic anion transporters using cDNA transfected cells (Hasegawa et al., 2003). In vivo studies in monkeys will further support the prediction of the occurrence of drug-drug interactions in humans. Nagata et al. (2004) found a drug-drug interaction involving rOat3 in the central nervous system (Nagata et al., 2004). Probenecid given as an i.v. constant infusion increased the concentrations of H_2 receptor antagonists (also given as an i.v. constant infusion) in the cerebrospinal fluid by inhibiting OAT3-mediated efflux at the choroid plexus. The possibility of drug-drug interactions with probenecid involving efflux transport across the barriers of the central nervous system can be also examined in monkeys in future studies.

In conclusion, the drug-drug interactions between the H_2 receptor antagonists (famotidine and cimetidine) and probenecid can be reproduced in monkeys. Hence, a combination of in vitro and in vivo studies could be a useful screening system for evaluating drug-drug interactions involving renal tubular transport in humans.

Acknowledgments

We thank Takashi Saito and Atsuko Takami (Pharmaceutical Research Institute, Kyowa Hakko Kogyo, Shizuoka, Japan) for helping with the monkey pharmacokinetic study.

References

Boom SP, Hoet S, and Russel FG (1997) Saturable urinary excretion kinetics of famotidine in the dog. *J Pharm Pharmacol* **49**:288–292.

Cunningham RF, Israili ZH, and Dayton PG (1981) Clinical pharmacokinetics of probenecid. *Clin Pharmacokinet* **6**:135–151.

Dedrick R, Bischoff KB, and Zaharko DS (1970) Interspecies correlation of plasma concentration history of methotrexate (NSC-740). *Cancer Chemother Rep* **54**:95–101.

Gisclon LG, Boyd RA, Williams RL, and Giacomini KM (1989) The effect of probenecid on the renal elimination of cimetidine. *Clin Pharmacol Ther* **45**:444–452.

Gladziwa U and Klotz U (1993) Pharmacokinetics and pharmacodynamics of H2-receptor antagonists in patients with renal insufficiency. *Clin Pharmacokinet* **24**:319–332.

Hasegawa M, Kusuhara H, Endou H, and Sugiyama Y (2003) Contribution of organic anion transporters to the renal uptake of anionic compounds and nucleoside derivatives in rat. *J Pharmacol Exp Ther* **305**:1087–1097.

Inotsume N, Nishimura M, Nakano M, Fujiyama S, and Sato T (1990) The inhibitory effect of probenecid on renal excretion of famotidine in young, healthy volunteers. *J Clin Pharmacol* **30**:50–56.

Kroemer H and Klotz U (1987) Pharmacokinetics of famotidine in man. *Int J Clin Pharmacol Ther Toxicol* **25**:458–463.

Lee W and Kim RB (2004) Transporters and renal drug elimination. *Annu Rev Pharmacol Toxicol* **44**:137–166.

Lin JH (1995) Species similarities and differences in pharmacokinetics. *Drug Metab Dispos* **23**:1008–1021.

Lin JH, Los LE, Ulm EH, and Duggan DE (1987) Urinary excretion kinetics of famotidine in rats. *Drug Metab Dispos* **15**:212–216

Lin JH, Los LE, Ulm EH, and Duggan DE (1988) Kinetic studies on the competition between famotidine and cimetidine in rats: evidence of multiple renal secretory systems for organic cations. *Drug Metab Dispos* **16**:52–56.

Mahmood I (1998) Interspecies scaling of renally secreted drugs. *Life Sci* **63**:2365–2371.

Matsushita H, Suzuki H, Sugiyama Y, Sawada Y, Iga T, Hanano M, and Kawaguchi Y (1990) Prediction of the pharmacokinetics of cefodizime and cefotetan in human from pharmacokinetic parameters in animals. *J Pharmacobiodyn* **13**:602–611.

Miyazaki H, Sekine T, and Endou H (2004) The multispecific organic anion transporter family: properties and pharmacological significance. *Trends Pharmacol Sci* **25**:654–662.

Motohashi H, Sakurai Y, Saito H, Masuda S, Urakami Y, Goto M, Fukatsu A, Ogawa O, and Inui K (2002) Gene expression levels and immunolocalization of organic ion transporters in the human kidney. *J Am Soc Nephrol* **13**:866–874.

Nagata Y, Kusuhara H, Hirono S, Endou H, and Sugiyama Y (2004) Carrier-mediated uptake of H2-receptor antagonists by the rat choroid plexus: involvement of rat organic anion transporter 3. *Drug Metab Dispos* **32**:1040–1047.

Reigner BG, Williams PE, Patel IH, Steimer JL, Peck C, and van Brummelen P (1997) An evaluation of the integration of pharmacokinetic and pharmacodynamic principles in clinical drug development: experience within Hoffmann La Roche. *Clin Pharmacokinet* **33**:142–152.

Shitara Y, Sato H, and Sugiyama Y (2005) Evaluation of drug-drug interaction in the hepatobiliary and renal transport of drugs. *Annu Rev Pharmacol Toxicol* **45**:689–723.

Slitt AL, Cherrington NJ, Hartley DP, Leazer TM, and Klaassen CD (2002) Tissue distribution and renal developmental changes in rat organic cation transporter mRNA levels. *Drug Metab Dispos* **30**:212–219.

Tahara H, Kusuhara H, Endou H, Koepsell H, Imaoka T, Fuse E, and Sugiyama Y (2005a) A species difference in the transport activities of H_2 receptor antagonists by rat and human renal organic anion and cation transporters. *J Pharmacol Exp Ther* **315**:1–9.

Tahara H, Shono M, Kusuhara H, Kinoshita H, Fuse E, Takadate A, Otagiri M, and Sugiyama Y (2005b) Molecular cloning and functional analyses of OAT1 and OAT3 from cynomolgus monkey kidney. *Pharm Res (NY)* **22**:647–660.

Ward KW and Smith BR (2004a) A comprehensive quantitative and qualitative evaluation of extrapolation of intravenous pharmacokinetic parameters from rat, dog and monkey to human: I. Clearance. *Drug Metab Dispos* **32**:603–611.

Ward KW and Smith BR (2004b) A comprehensive quantitative and qualitative evaluation of extrapolation of intravenous pharmacokinetic parameters from rat, dog and monkey to human: II. Volume of distribution and mean residence time. *Drug Metab Dispos* **32**:612–619.

Wright SH and Dantzler WH (2004) Molecular and cellular physiology of renal organic cation and anion transport. *Physiol Rev* **84**:987–1049.

Yamaoka K, Tanigawara Y, Nakagawa T, and Uno T (1981) A pharmacokinetic analysis program (multi) for microcomputer. *J Pharmacobiodyn* **4**:879–885.

Address correspondence to: Dr. Yuichi Sugiyama, Graduate School of Pharmaceutical Sciences, University of Tokyo, Hongo, Bunkyo-ku, Tokyo, 113-0033, Japan. E-mail: sugiyama@mol.f.u-tokyo.ac.jp

0090-9556/06/3407-1229–1236$20.00
DRUG METABOLISM AND DISPOSITION
Copyright © 2006 by The American Society for Pharmacology and Experimental Therapeutics
DMD 34:1229–1236, 2006

Vol. 34, No. 7
9290/3119191
Printed in U.S.A.

DRUG-DRUG INTERACTION BETWEEN PITAVASTATIN AND VARIOUS DRUGS VIA OATP1B1

Masaru Hirano, Kazuya Maeda, Yoshihisa Shitara, and Yuichi Sugiyama

Graduate School of Pharmaceutical Sciences, the University of Tokyo, Tokyo, Japan (M.H., K.M., Y.Su.); and Graduate School of Pharmaceutical Sciences, Chiba University, Chiba, Japan (Y.Sh.)

Received January 6, 2006; accepted March 29, 2006

ABSTRACT:

It has already been demonstrated that pitavastatin, a novel potent HMG-coenzyme A reductase inhibitor, is taken up into human hepatocytes mainly by organic anion transporting polypeptide (OATP) 1B1. Because OATP2B1 is also localized in the basolateral membrane of human liver, we took two approaches to further confirm the minor contribution of OATP2B1 to the hepatic uptake of pitavastatin. Western blot analysis revealed that the ratio of the band density of OATP2B1 in human hepatocytes to that in our expression system is at least 6-fold lower compared with OATP1B1 and OATP1B3. The uptake of pitavastatin in human hepatocytes could be inhibited by both estrone-3-sulfate (OATP1B1/OATP2B1 inhibitor) and estradiol-17β-D-glucuronide (OATP1B1/OATP1B3 inhibitor). These results further supported the idea that OATP1B1 is a predominant transporter for the hepatic uptake of pitavastatin. Then, to explore the possibility of OATP1B1-mediated drug-drug interaction, we checked the inhibitory effects of various drugs on the pitavastatin uptake in OATP1B1-expressing cells and evaluated whether the in vitro inhibition was clinically significant or not. As we previously reported, we used the methodology for estimating the maximum unbound concentration of inhibitors at the inlet to the liver ($I_{u,in,max}$). Judging from $I_{u,in,max}$ and inhibition constant (K_i) for OATP1B1, several drugs (especially cyclosporin A, rifampicin, rifamycin SV, clarithromycin, and indinavir) have potentials for interacting with OATP1B1-mediated uptake of pitavastatin. The in vitro experiments could support the clinically observed drug-drug interaction between pitavastatin and cyclosporin A. These results suggest that we should pay attention to the concomitant use of some drugs with pitavastatin.

The liver is one of the organs responsible for the elimination of xenobiotics including many kinds of drugs. In some cases, although the compounds were not supposed to easily penetrate the plasma membrane from the viewpoint of their physicochemical properties, they were efficiently taken up into liver and excreted into bile. Recently, it has been found that several kinds of transporters greatly help the efficient membrane transport of several compounds. It has been characterized that hepatic uptake of some of the compounds is mediated by organic anion-transporting polypeptide (OATP) family transporters, organic anion transporter 2, Na^+-taurocholate cotransporting polypeptide, and organic cation transporter 1 (Mizuno et al., 2003). Among these transporters, especially OATP1B1 and OATP1B3 are specifically expressed in liver and show broad substrate specificities (Hagenbuch and Meier, 2003). In contrast, OATP2B1 is also expressed in the basolateral membrane of human liver (Tamai et al., 2001). Previous reports indicated that the low pH facilitates the OATP2B1-mediated uptake of several organic anions, implying its involvement in the intestinal absorption of anions (Kobayashi et al., 2003). Although the uptake clearance at pH 7.4 was lower than that at pH 5.0, OATP2B1 could transport some organic anions such as estrone-3-sulfate, fexofenadine, benzylpenicillin, and dehydroepiandrosterone sulfate, even at pH 7.4 (Kobayashi et al., 2003; Nozawa et al., 2004). Therefore, it is possible that OATP2B1 is also involved in the hepatic uptake of anionic drugs.

Pitavastatin is a highly potent inhibitor of HMG-coenzyme A reductase, the rate-limiting enzyme in cholesterol biosynthesis (Aoki et al., 1997; Kajinami et al., 2003). Previously, Kimata et al. (1998) have revealed that [^{14}C]pitavastatin is selectively distributed to the liver in rats with the liver-to-plasma concentration ratio of more than 50, suggesting that active transport systems can be involved in the uptake of pitavastatin. We have already demonstrated that pitavastatin is taken up into human hepatocytes predominantly by OATP1B1, although it was a substrate of both OATP1B1 and OATP1B3 (Hirano et al., 2004). We also showed that the contribution of other transporters such as OATP2B1 to the pitavastatin uptake was theoretically small, but we have not experimentally shown the minor importance of OATP2B1. Therefore, we tried to confirm that OATP1B1 is a responsible transporter for the pitavastatin uptake by two kinds of approaches: the comparison of the expression level of each transporter in human hepatocytes and expression systems by Western blot analysis, and the inhibitory effects of transporter-selective inhibitors on the uptake of pitavastatin in human hepatocytes.

This work was supported by Health and Labour Sciences Research Grants from the Ministry of Health, Labour and Welfare for the Research on Advanced Medical Technology and a Grant-in Aid for Young Scientists (B) (15790087) from the Ministry of Education, Culture, Sports, Science and Technology.

Article, publication date, and citation information can be found at http://dmd.aspetjournals.org.

doi:10.1124/dmd.106.009290.

ABBREVIATIONS: HEK, human embryonic kidney; MDCK, Madin-Darby canine kidney; OATP, organic anion-transporting polypeptide; HMG-CoA, 3-hydroxy-3-methylglutaryl-coenzyme A; K_m, Michaelis constant; V_{max}, maximum transport velocity; K_i, inhibition constant; $E_2$17βG, estradiol 17β-D-glucuronide; E_1S, estrone-3-sulfate; DDI, drug-drug interaction.

The combination therapy of statins and various compounds is widely used in clinical practice. Coadministration of various drugs sometimes causes an increase in the plasma concentration of statins (Williams and Feely, 2002), which may occasionally lead to severe side effects such as myopathy and rhabdomyolysis (Evans and Rees, 2002). In the case of simvastatin, which is relatively lipophilic and metabolized by CYP3A4, itraconazole, cyclosporin A, and erythromycin were reported to increase plasma area under the plasma concentration-time curve of simvastatin by inhibition of CYP3A4-mediated metabolism (Kantola et al., 1998; Neuvonen et al., 1998; Ichimaru et al., 2001). In contrast, cyclosporin A also interacted with the nonmetabolized type of statins such as pravastatin, pitavastatin, and rosuvastatin in the clinical situation (Olbricht et al., 1997; Hasunuma et al., 2003; Simonson et al., 2004). Shitara et al. (2003) clarified that drug-drug interaction (DDI) between cyclosporin A and cerivastatin is caused by the inhibition of OATP1B1-mediated cerivastatin uptake by cyclosporin A. Because pitavastatin was reported to be taken up into hepatocytes mainly by OATP1B1 (Hirano et al., 2004), we should pay attention to the OATP1B1-mediated DDI of pitavastatin in coadministration with other drugs that can inhibit the function of OATP1B1. However, the inhibitors of OATP1B1 identified by in vitro analyses do not always cause DDI in the clinical situation when the clinical protein unbound concentration in plasma is much lower than the in vitro inhibition constant (K_i) for OATP1B1. Ito et al. (1998) proposed the calculation method for estimating the maximum unbound concentration of inhibitors at the inlet to the liver to avoid the false-negative prediction of clinical DDI.

In the present study, we confirmed the minor contribution of OATP2B1 to the hepatic uptake of pitavastatin by two approaches. Moreover, we tried to predict the possible DDI mediated by OATP1B1 between pitavastatin and various drugs by judging from the clinical maximum unbound concentration of each inhibitor in human plasma and the K_i value for OATP1B1 obtained from the in vitro study.

Materials and Methods

Materials. Pitavastatin, monocalcium bis[(3*R*,5*S*,6*E*)-7-[2-cyclopropyl-4-(4-fluorophenyl)-3-quinolyl]3,5-dihydroxy-6-hepteonate], was synthesized by Nissan Chemical Industries (Chiba, Japan). [^{3}H]Pitavastatin (16.0 Ci/mmol) was synthesized by GE Healthcare (Little Chalfont, Buckinghamshire, UK). [^{3}H]Estradiol 17β-D-glucuronide ($E_2$17βG) and [^{3}H]estrone-3-sulfate (E_1S) (45 Ci/mmol and 46 Ci/mmol, respectively) were purchased from New England Nuclear (Boston, MA). Unlabeled $E_2$17βG, E_1S, and gemfibrozil were purchased from Sigma-Aldrich (St. Louis, MO). A metabolite of gemfibrozil, M3 (purity 99.6%), was chemically synthesized at KNC Laboratories, Co. Ltd. (Kobe, Japan) as shown in detail previously (Shitara et al., 2004). All other chemicals were of analytical grade and commercially available.

Uptake Study Using Transporter Expression Systems. OATP1B1-, OATP1B3-, and OATP2B1-expressing HEK293 cells and vector-transfected control cells used in this study were constructed previously (Hirano et al., 2004; Shimizu et al., 2005). Transporter-expressing or vector-transfected HEK293 cells were grown in Dulbecco's modified Eagle's medium low glucose (Invitrogen, Carlsbad, CA) supplemented with 10% fetal bovine serum (Sigma-Aldrich), 100 U/ml penicillin, 100 μg/ml streptomycin, and 0.25 μg/ml amphotericin B at 37°C with 5% CO_2 and 95% humidity. Cells were then seeded in 12-well plates coated with poly-L-lysine/poly-L-ornithine at a density of 1.5×10^5 cells per well. After 2 days, the cell culture medium was replaced with culture medium supplemented with 5 mM sodium butyrate 24 h before transport assay to induce the expression of exogenous transporters. The transport study was carried out as described previously (Sugiyama et al., 2001). Uptake was initiated by adding Krebs-Henseleit buffer containing radiolabeled and unlabeled substrates after cells had been washed twice and preincubated with Krebs-Henseleit buffer at 37°C for 15 min. The Krebs-Henseleit buffer consisted of 118 mM NaCl, 23.8 mM $NaHCO_3$, 4.8 mM KCl, 1.0 mM KH_2PO_4, 1.2 mM $MgSO_4$, 12.5 mM HEPES, 5.0 mM glucose, and 1.5 mM $CaCl_2$ adjusted to pH 7.4. The uptake was terminated at a designated time by adding ice-cold Krebs-Henseleit buffer after removal of the incubation buffer. Then, cells were washed twice with 1 ml of ice-cold Krebs-Henseleit buffer, solubilized in 500 μl of 0.2 N NaOH, and kept overnight at 4°C. Aliquots (500 μl) were transferred to scintillation vials after adding 250 μl of 0.4 N HCl. The radioactivity associated with the cells and incubation buffer was measured in a liquid scintillation counter (LS6000SE; Beckman Coulter, Inc., Fullerton, CA) after adding 2 ml of scintillation fluid (Clear-sol I; Nacalai Tesque, Kyoto, Japan) to the scintillation vials. The remaining 50 μl of cell lysate was used to determine the protein concentration by the method of Lowry et al. (1951) with bovine serum albumin as a standard.

Uptake Study Using Human Cryopreserved Hepatocytes. This experiment was performed as described previously (Shitara et al., 2003). Cryopreserved human hepatocytes were purchased from In Vitro Technologies (Baltimore, MD). In this experiment, we selected three batches of human hepatocytes (lots OCF, 094, and ETR), which ranked in the top three of the uptake amount of $E_2$17βG, and E_1S among eight independent batches of hepatocytes. Immediately before the study, the hepatocytes (1-ml suspension) were thawed at 37°C, quickly suspended in 10 ml of ice-cold Krebs-Henseleit buffer, and centrifuged (50*g*) for 2 min at 4°C, followed by removal of the supernatant. This procedure was repeated once more to remove cryopreservation buffer, and then the cells were resuspended in the same buffer to give a cell density of 1.0×10^6 viable cells/ml for the uptake study. The number of viable cells was determined by trypan blue staining. Before the uptake studies, the cell suspensions were prewarmed in an incubator at 37°C for 3 min. The uptake studies were initiated by adding an equal volume of buffer containing radiolabeled and unlabeled pitavastatin to the cell suspension. After incubation at 37°C for 0.5 and 2 min, the reaction was terminated by separating the cells from the buffer. For this purpose, an aliquot of 80 μl of incubation mixture was collected and placed in a centrifuge tube (450 μl) containing 50 μl of 2 N NaOH under a layer of 100 μl of oil (density, 1.015; a mixture of silicone oil and mineral oil; Sigma-Aldrich), and subsequently the sample tube was centrifuged for 10 s using a tabletop centrifuge (10,000*g*; Beckman Microfuge E; Beckman Coulter, Inc.). During this process, hepatocytes passed through the oil layer into the alkaline solution. After an overnight incubation in alkali to dissolve the hepatocytes, the centrifuge tube was cut and each compartment was transferred to a scintillation vial. The compartment containing the dissolved cells was neutralized with 50 μl of 2 N HCl, mixed with scintillation cocktail, and the radioactivity was measured in a liquid scintillation counter.

Antiserum and Western Blot Analysis. As shown in previous reports, anti-OATP2B1 sera were raised in rabbits against a synthetic peptide consisting of the 15 carboxyl-terminal amino acids of OATP2B1 (LLVSGPGKKPEDSRV) coupled to keyhole limpet hemocyanine at its N-terminal via an additional cysteine (Kullak-Ublick et al., 2001). Crude membrane fractions were prepared from human hepatocytes and transporter-expressing HEK293 cells as described previously (Sasaki et al., 2002). The human liver block (lot 020188) was obtained from Human and Animal Bridging Research Organization (Chiba, Japan), and crude membrane fractions were prepared as described previously (Hirano et al., 2004). The samples were diluted with 3× Red loading buffer (BioLabs, Hertfordshire, UK) and loaded onto a 7% SDS-polyacrylamide gel with a 4.4% stacking gel. Proteins were electroblotted onto a polyvinylidene difluoride membrane (Pall, East Hills, NY) using a blotter (Trans-blot; Bio-Rad, Richmond, CA) at 15 V for 1 h. The membrane was blocked with Tris-buffered saline containing 0.05% Tween 20 (TBS-T) and 5% skimmed milk for 1 h at room temperature. After washing with TBS-T, the membrane was incubated with anti-OATP2B1 serum (dilution 1:1000). The membrane was incubated with a horseradish peroxidase-labeled anti-rabbit IgG antibody (GE Healthcare) diluted 1:5000 in TBS-T for 1 h at room temperature, followed by washing with TBS-T. The band was detected and its intensity was quantified using an image analyzer (LAS-1000 plus; Fuji Film, Tokyo, Japan).

Transcellular Transport Study. OATP1B1-, OATP1B1/BCRP-, OATP1B1/MDR1-, and OATP1B1/MRP2-expressing MDCKII cells and vector-transfected control cells used in this study were constructed previously (Matsushima et al., 2005). Transporter-expressing or vector-transfected MDCKII cells were grown in Dulbecco's modified Eagle's medium low glucose supplemented with 10% fetal bovine serum, 100 U/ml penicillin, 100

μg/ml streptomycin, and 0.25 μg/ml amphotericin B at 37°C with 5% CO_2 and 95% humidity. MDCKII cells were seeded on Transwell membrane inserts (6.5-mm diameter, 0.4-μm pore size; Corning Costar, Bodenheim, Germany) at a density of 1.4×10^5 cells per well. After 3 days, medium was replaced with 5 mM sodium butyrate for 24 h before the transport study (Sasaki et al., 2002). The experiments were initiated by replacing the medium on the basal side of the cell layer with Krebs-Henseleiti buffer containing radiolabeled and unlabeled pitavastatin (0.3 μM). The cells were incubated at 37°C, and aliquots of medium were taken from each compartment at designated time points. Radioactivity in 100 μl of medium was measured in a liquid scintillation counter after the addition of scintillation cocktail. At the end of the experiments, the cells were washed three times with 1.5 ml of ice-cold Krebs-Henseleit buffer and solubilized in 500 μl of 0.2 N NaOH. After addition of 100 μl of 1 N HCl, 500-μl aliquots were transferred to scintillation vials. Aliquots (50-μl) of cell lysate were used to determine protein concentrations as described above. To evaluate the efflux transport clearance via recombinant BCRP, MDR1, and MRP2 in the double transfectants, the apparent efflux clearance across the apical membrane (PS_{apical}) was calculated by dividing the steady-state velocity for the transcellular transport ($V_{transcellular}$) of pitavastatin, determined over 3 h, by the intracellular concentration (C_{cell}) of pitavastatin, determined at the end of the experiments (3 h) in the absence or presence of the inhibitors.

$$PS_{apical} = V_{transcellular}/C_{cell} \quad (1)$$

Kinetic Analyses. Ligand uptake in transporter cDNA-transfected cells was expressed as the uptake volume (μl/mg protein), given as the amount of radioactivity associated with the cells (dpm/mg protein) divided by its concentration in the incubation medium (dpm/μl). Transporter-specific uptake was obtained by subtracting the uptake into vector-transfected cells from the uptake into cDNA-transfected cells. Kinetic parameters were obtained using the following equation:

$$v = \frac{V_{max} \times S}{K_m + S} + P_{dif} \times S \quad (2)$$

where v is the uptake velocity of the substrate (pmol/min/mg protein), S is the substrate concentration in the medium (μM), K_m is the Michaelis constant (μM), V_{max} is the maximum uptake rate (pmol/min/mg protein), and P_{dif} is the nonsaturable uptake clearance (μl/min/mg protein). The Damping Gauss-Newton Method algorithm was used with a MULTI program (Yamaoka et al., 1981) to perform nonlinear least-squares data fitting. The input data were weighted as the reciprocal of the observed values. Inhibition constants (K_i) of a series of compounds could be calculated by the following equation, if the substrate concentration was low enough compared with its K_m value.

$$CL(+I) = \frac{CL}{1 + \frac{I}{K_i}} \quad (3)$$

where CL represents the uptake clearance in the absence of inhibitor, $CL(+I)$ represents the uptake clearance in the presence of inhibitor, and I represents the inhibitor concentration. When fitting the data to determine the K_i value, the input data were weighed as the reciprocal of the observed values.

To determine saturable hepatic uptake clearance in human hepatocytes, we first determined the hepatic uptake clearance ($CL_{(2\ min-0.5\ min)}$) (μl/min/10^6 cells) by calculating the slope of the uptake volume (V_d) (μl/10^6 cells) between 0.5 and 2 min as shown previously (Hirano et al., 2004) (eq. 4). The saturable component of the hepatic uptake clearance (CL_{hep}) was determined by subtracting $CL_{(2\ min-0.5\ min)}$ in the presence of 100 μM substrate (excess) from that in the presence of 0.1 μM substrate (tracer) (eq. 5).

$$CL_{(2\ min-0.5\ min)} = \frac{V_{d,2\ min} - V_{d,0.5\ min}}{2 - 0.5} \quad (4)$$

$$CL_{hep} = CL_{(2\ min-0.5\ min),tracer} - CL_{(2\ min-0.5\ min),excess} \quad (5)$$

where $CL_{(2\ min-0.5\ min),tracer}$ and $CL_{(2\ min-0.5\ min),excess}$ represent $CL_{(2\ min-0.5\ min)}$ estimated in the presence of 0.1 and 100 μM substrate, respectively.

Estimation of the Contribution of Transporters to the Hepatic Uptake in Human Hepatocytes by Western Blot Analysis. The ratio of the expression level of each transporter in human hepatocytes (per 10^6 cells) to that in the expression system (per mg protein) was calculated by the intensity of specific bands in Western blot analysis and defined as R_{exp} as shown previously (Hirano et al., 2004). The uptake clearance by each transporter in human hepatocytes was separately calculated by multiplying the uptake clearance of the pitavastatin in transporter-expressing cells (CL_{test}) by R_{exp} as described in the following equation:

$$CL_{hep,test} = CL_{test} \cdot R_{exp} \quad (6)$$

The relative contribution (percentage) of each transporter to the uptake in human hepatocytes was defined by the ratio of $CL_{hep,test}$ for target transporter to that of the sum of $CL_{hep,test}$ for OATP1B1, OATP1B3, and OATP2B1.

Prediction of Clinical DDI between Pitavastatin and Various Drugs via OATP1B1. The degree of inhibition of OATP1B1 in humans was estimated by calculating the following R values, which represent the ratio of the uptake clearance in the absence of inhibitor to that in its presence:

$$R = 1 + \frac{f_u \cdot I_{in,max}}{K_i} \quad (7)$$

where f_u represents the blood unbound fraction of the inhibitor, $I_{in,max}$ represents the estimated maximum inhibitor concentration at the inlet to the liver, and K_i was obtained in the present in vitro study using OATP1B1-expressing HEK293 cells. For the estimation of R value, $I_{in,max}$ was calculated by the method of Ito et al. (1998):

$$I_{in,max} = I_{max} + \frac{F_a \cdot Dose \cdot k_a}{Q_h} \quad (8)$$

where I_{max} represents the reported value for the maximum plasma concentration in the systemic circulation in the clinical situation, F_a represents the absorbed fraction of inhibitor, k_a is the absorption rate constant in the intestine, and Q_h represents the hepatic blood flow rate in humans (1610 ml/min). To estimate the maximum $I_{in,max}$ value, F_a was set at 1, k_a was set at 0.1 min^{-1} [minimum gastric emptying time (10 min)], and the blood-to-plasma concentration ratio was assumed to be 1, if the information from the literature was not available.

Results

Uptake of E_1S and Pitavastatin by OATP2B1-Expressing Cells. The time profiles and Eadie-Hofstee plots of the uptake of E_1S and pitavastatin by OATP2B1-expressing and vector-transfected HEK293 cells are shown in Fig. 1. Pitavastatin as well as E_1S was significantly taken up into OATP2B1-expressing HEK293 cells compared with vector-transfected cells (Fig. 1, A and B). The saturation kinetics of their uptake is shown in Fig. 1, C and D. The concentration dependence of the uptake of E_1S could be explained by a one-saturable component (Fig. 1C). The K_m and V_{max} values for the OATP2B1-mediated uptake of E_1S were 20.9 ± 2.0 μM and 1196 ± 40 pmol/min/mg protein, respectively. The nonsaturable component was observed in the Eadie-Hofstee plot even for the specific uptake of pitavastatin by OATP2B1 (Fig. 1D). The K_m and V_{max} values of pitavastatin for the saturable component and uptake clearance for the nonsaturable component were 1.17 ± 0.28 μM, 7.36 ± 1.43 pmol/min/mg protein, and 2.93 ± 0.16 μl/min/mg protein, respectively. No significant uptake of $E_2 17\beta G$ by OATP2B1 could be observed (7.51 ± 0.49 and 9.72 ± 1.29 μl/mg protein by vector-transfected and OATP2B1-expressing cells for 5 min, respectively; $n = 3$).

Western Blot Analysis of OATP2B1. The relative expression level of OATP2B1 in crude membrane from transfectants and human hepatocytes was estimated by Western blot analyses. An antiserum against OATP2B1 recognized approximately 85-kDa proteins in the crude membrane fractions prepared from human hepatocytes and OATP2B1-expressing cells (Fig. 2A). The molecular weight of OATP2B1 in human hepatocytes was almost the same as that pre-

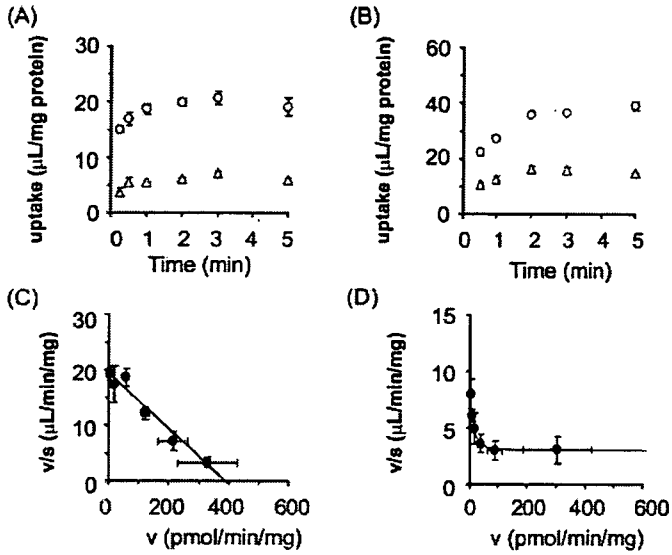

FIG. 1. Time profiles and Eadie-Hofstee plots of the uptake of [^{3}H]E_1S and [^{3}H]pitavastatin by OATP2B1-expressing HEK293 cells. The uptake of 0.1 μM [^{3}H]E_1S (A) and 0.1 μM [^{3}H]pitavastatin (B) by cDNA-transfected cells was examined at 37°C. Open circles and triangles represent the uptake in OATP2B1-expressing HEK293 cells and vector-transfected control cells, respectively. The concentration dependence of OATP2B1-mediated uptake of [^{3}H]E_1S (C) and [^{3}H]pitavastatin (D) is shown as Eadie-Hofstee plots. Closed circles represent the OATP2B1-mediated specific uptake rate, which was obtained by subtracting the initial uptake rate in vector-transfected cells from that in OATP2B1-expressing cells. The initial uptake rate calculated from the uptake of [^{3}H]E_1S and [^{3}H]pitavastatin for 1 and 2 min, respectively, was determined at various concentrations (0.3–100 μM). Solid lines represent the fitted curves obtained by nonlinear regression analysis. Each point represents the mean ± S.E. (n = 3). Where error bars are not shown, the S.E. values are within the limits of the symbol.

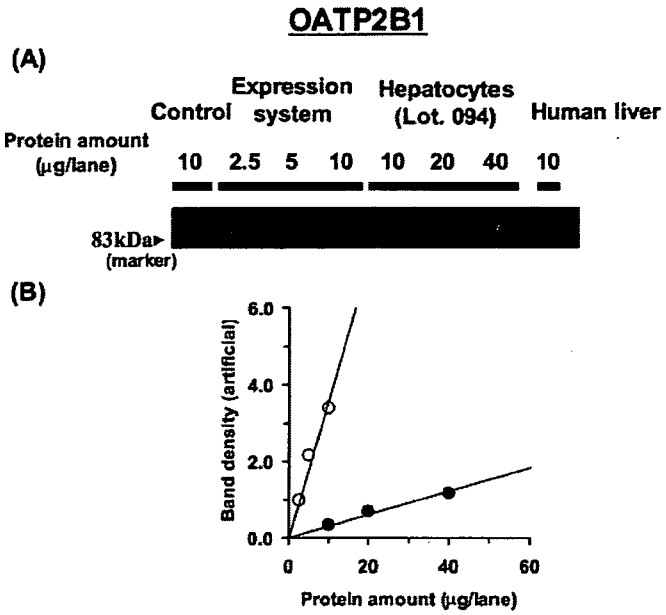

FIG. 2. Western blot analysis of OATP2B1. A, crude membrane fractions (2.5–40 μg) prepared from OATP2B1-expressed HEK293 cells and human hepatocytes (lot 094) were loaded and separated by SDS-polyacrylamide gel electrophoresis (7% separating gel). The sample designated as "Human liver" indicates that the crude membrane vesicles were prepared from a human frozen liver block (lot 020188) as a positive control. OATP2B1 was detected by preimmune antisera raised against the carboxyl terminus of human OATP2B1. B, comparison of the relative expression levels of OATP2B1 between transfectants and hepatocytes is shown. The x and y axes represent the amount of crude membrane obtained from transfectants and human hepatocytes and the intensity of the specific band in Western blot analysis, respectively. Closed circles and open circles indicate the band density of human hepatocytes (lot 094) and OATP2B1-expressing HEK293 cells, respectively. The solid lines represent the fitted lines obtained by linear regression analysis.

pared from human liver block, but was slightly lower than that in OATP2B1-expressing HEK293 cells. No specific band of OATP2B1 was detected in vector-transfected cells. Figure 2B showed the linear relationship between the applied protein amount of crude membrane obtained from OATP2B1-expressing cells and human hepatocytes and the intensity of the specific band measured by digital densitometer. The slope of the regression line in Fig. 2B reflected the relative expression level of OATP2B1 in transfectants and hepatocytes.

Estimation of Contribution of OATP1B1, OATP1B3, and OATP2B1 in Human Hepatocytes by Western Blot Analysis. We calculated the estimated uptake clearance of pitavastatin by OATP1B1, OATP1B3, and OATP2B1 in human hepatocytes by the relative expression level of each transporter (Table 1). We obtained 62.1 μg of protein in crude membrane from 1 mg of whole cell protein in OATP2B1-expressing HEK293 cells, whereas 178, 89, and 82 μg of protein were obtained in crude membrane from 10^6 human hepatocytes of lot OCF, 094, and ETR, respectively. When the band density per unit protein amount in crude membrane of OATP2B1-expressing HEK293 cells is defined as 1, the relative expression levels of OATP2B1 per unit protein amount in crude membrane of hepatocytes of lots OCF, 094, and ETR are 0.200, 0.152, and 0.112 (per microgram), respectively. Using these R_{exp} values and our previous results (Hirano et al., 2004; shown in Table 1), we estimated the relative contribution of OATP1B1, OATP1B3, and OATP2B1 to the hepatic uptake of pitavastatin in human hepatocytes.

Inhibitory Effects of $E_2$17βG and E_1S on the Uptake of Pitavastatin by Transporter-Expression System and Human Hepatocytes. Inhibitory effects of $E_2$17βG and E_1S on the uptake of pitavastatin were examined by human cryopreserved hepatocytes (Fig. 3). $E_2$17βG (100 μM) inhibited OATP1B1- and OATP1B3-mediated transport of pitavastatin to 10.0 ± 3.2 and 21.7 ± 8.7% of control, respectively (n = 3), whereas OATP2B1-mediated transport was not affected by 100 μM $E_2$17βG (91.8 ± 16.6%). In contrast, 100 μM E_1S inhibited OATP1B1- and OATP2B1-mediated transport of pitavastatin to 7.19 ± 2.94 and 56.5 ± 3.2% of control, respectively (n = 3), whereas OATP1B3-mediated transport was not affected by 100 μM E_1S (102 ± 7%). In three batches of human hepatocytes, pitavastatin uptake was almost inhibited by 100 μM $E_2$17βG (Fig. 3A) and E_1S (Fig. 3B).

Prediction of DDI between Pitavastatin and Various Compounds by OATP1B1-Expressing HEK293 Cells. To identify clinically relevant inhibitors for OATP1B1-mediated pitavastatin uptake, inhibitory effects of several compounds on the uptake of pitavastatin were determined by OATP1B1-expressing cells. These compounds include therapeutic agents that were reported to cause DDI with statins (Williams and Feely, 2002). Cyclosporin A, fenofibrate, gemfibrozil, and gemfibrozil metabolites (gemfibrozil-M3 and gemfibrozil-1-*O*-glucuronide) were also investigated because drug interaction studies with pitavastatin have been previously reported (Hasunuma et al., 2003; Mathew et al., 2004). Most of the compounds we tested could inhibit OATP1B1-mediated pitavastatin uptake (Table 2). We also obtained the blood unbound fraction (f_u) and calculated the estimated maximum concentration at the inlet to the liver ($I_{in,max}$) of the inhibitors from the literature information (Clark et al., 1992; Hardman et al., 2001; package insert of each drug). Inhibition constants (K_i) of various compounds for OATP1B1 obtained in the present study and the ratio of the uptake clearance in the absence of inhibitor to that in its presence (R value) are summarized in Table 2. R values of cyclosporin A, rifampicin, rifamycin SV, clarithromycin,

TABLE 1

Contribution of OATP1B1, OATP1B3, and OATP2B1 to the hepatic uptake of pitavastatin determined by the relative expression level

Hepatocyte Lot	Ratio of Expression Level[a] (Hepatocyte/Expression System)			Estimated Clearance[b]		
	$R_{exp,OATP1B1}$	$R_{exp,OATP1B3}$	$R_{exp,OATP2B1}$	OATP1B1	OATP1B3	OATP2B1
					μl/min/10⁶ cells	
OCF	2.90[c]	1.21[c]	0.200	222	37.0	0.658
				85.5%	14.3%	0.253%
094	1.58[c]	0.930[c]	0.152	121	28.5	0.500
				80.7%	19.0%	0.333%
ETR	0.890[c]	0.737[c]	0.112	68.2	22.6	0.368
				74.8%	24.8%	0.405%

[a] Ratio of the expression level was determined by the intensity of the specific band in the crude membrane prepared from human hepatocytes (per 10^6 cells) divided by that in the crude membrane from transporter-expressing cells (per milligram) in Western blot analysis.

[b] In the 'Estimated Clearance' column, each percentage value indicates the percentage of the OATP1B1-, OATP1B3-, or OATP2B1-mediated uptake clearance relative to the sum of the estimated clearance mediated by OATP1B1, OATP1B3, and OATP2B1. The details of this estimation are described under *Materials and Methods*.

[c] Values from Hirano et al. (2004).

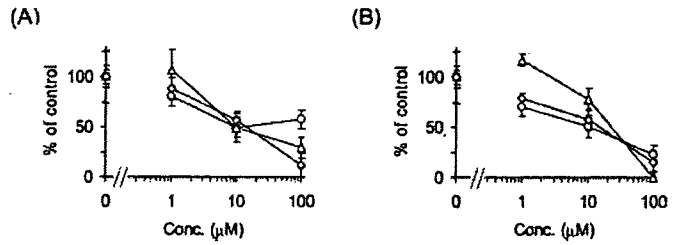

FIG. 3. Inhibitory effects of $E_2$17βG and E_1S on the uptake of [^{3}H]pitavastatin by human hepatocytes. The transport of [^{3}H]pitavastatin (0.1 μM) into human hepatocytes was determined in the presence or absence of $E_2$17βG (A) and E_1S (B) at the designated concentrations. Open circles, triangles, and squares represent the uptake in human hepatocytes of lots OCF, 094, and ETR, respectively. The detailed method for calculation of the uptake clearance in hepatocytes (CL_{hep}) is described under *Materials and Methods*. The values are expressed as a percentage of the uptake of [^{3}H]pitavastatin in the absence of inhibitors. Each point represents the mean ± S.E. (n = 3).

and indinavir were higher than 2.5, suggesting that these drugs can interact with pitavastatin in a clinical situation.

Inhibitory Effects of Cyclosporin A, Gemfibrozil, and Its Metabolites on the Transcellular Transport of Pitavastatin in OATP1B1/MRP2, OATP1B1/MDR1, and OATP1B1/BCRP Double Transfectants. The inhibitory effects of cyclosporin A, gemfibrozil, gemfibrozil-1-*O*-glucuronide, and gemfibrozil-M3 on the transcellular transport of pitavastatin were investigated in double-transfected cells. The transcellular transport clearance (PS_{net}) of pitavastatin was drastically decreased by cyclosporin A in all kinds of double transfectants (Fig. 4A). The efflux clearance from cells to the apical compartment (PS_{apical}) was also potently reduced by cyclosporin A (Fig. 5A). In contrast, gemfibrozil and gemfibrozil-1-*O*-glucuronide did not change either PS_{net} or PS_{apical} up to 100 μM (Figs. 4 and 5). Gemfibrozil-M3 (300 μM) could not inhibit the PS_{apical} of pitavastatin in OATP1B1/BCRP-, OATP1B1/MDR1-, and OATP1B1/MRP2-expressing MDCKII cells (data not shown). The K_i values of these inhibitors on the PS_{net} and PS_{apical} of pitavastatin are summarized in Table 3.

TABLE 2

The K_i values for OATP1B1-mediated pitavastatin uptake and the prediction of the possibility of DDI by considering the maximum plasma unbound concentration at the inlet to the liver

The K_i values are expressed as mean ± computer-calculated S.D. R value = 1 + $f_u \cdot I_{in,max}/K_i$.

Inhibitor	K_i Value for OATP1B1	R Value
	μM	
Cyclosporin A	0.242 ± 0.029	3.55
Tacrolimus	0.611 ± 0.069	1.20
Rifampicin	0.477 ± 0.030	13.4
Rifamycin SV	0.171 ± 0.024	65.6
Tolbutamide	>100	<1.21
Glibenclamide	0.746 ± 0.101	1.00
Fluconazole	>100	<1.25
Ketoconazole	19.2 ± 3.9	1.03
Itraconazole	>100	<1.00
Gemfibrozil	25.2 ± 4.7	1.08
Gemfibrozil-1-*O*-glucuronide	22.6 ± 5.8	1.10[a]
Gemfibrozil-M3	>300	<1.03[a]
Clofibrate	>300	<1.03
Ciprofibrate	141 ± 22	1.01
Bezafibrate	68.6 ± 11.9	1.03
Fenofibrate	>300	<1.00
Cimetidine	>300	<1.14
Ranitidine	>300	<1.16
Valsartan	8.96 ± 1.33	1.10
Telmisartan	0.436 ± 0.043	1.16
Chlorzoxazone	>100	<1.00
Colchichine	>100	<1.07
Phenytoin	>100	<1.03
Clarithromycin	8.26 ± 0.54	3.29
Erythromycin	11.4 ± 2.1	1.25
Indinavir	18.4 ± 1.9	2.77
Ritonavir	0.781 ± 0.048	2.25
Saquinavir	1.59 ± 0.13	1.62
Probenecid	76.2 ± 7.1	1.85
Methotrexate	>300	<1.01
Digoxin	31.7 ± 3.0	1.00
Diltiazem	>100	<1.03
Verapamil	51.6 ± 15.9	1.02
Warfarin	83.3 ± 9.7	1.00

[a] These values were calculated by using the reported values for the maximum plasma concentration of inhibitors in the clinical situations, instead of $I_{in,max}$, because we did not have enough parameters to estimate the $I_{in,max}$ value.

Discussion

In the present study, we have excluded the possibility of a major contribution of OATP2B1 to the hepatic uptake of pitavastatin and confirmed that OATP1B1 is the most important transporter for its uptake. Next, the inhibitory effects of pitavastatin uptake by several drugs in OATP1B1-expressing cells were also investigated, and we discussed the possibility of DDI in clinical stage by considering the inhibition constant (K_i) obtained from in vitro analysis and the estimated maximum unbound concentration of each inhibitor at the inlet to the liver.

We observed the significant saturable uptake of pitavastatin in OATP2B1-expressing cells compared with control cells at pH 7.4 with a K_m value of 1.17 μM (Fig. 1). It has been shown that specific uptake of pravastatin by OATP2B1 was not significantly observed at pH 7.4, whereas it can be transported at pH 5.0 (Nozawa et al., 2004), indicating that pitavastatin is preferentially recognized by OATP2B1

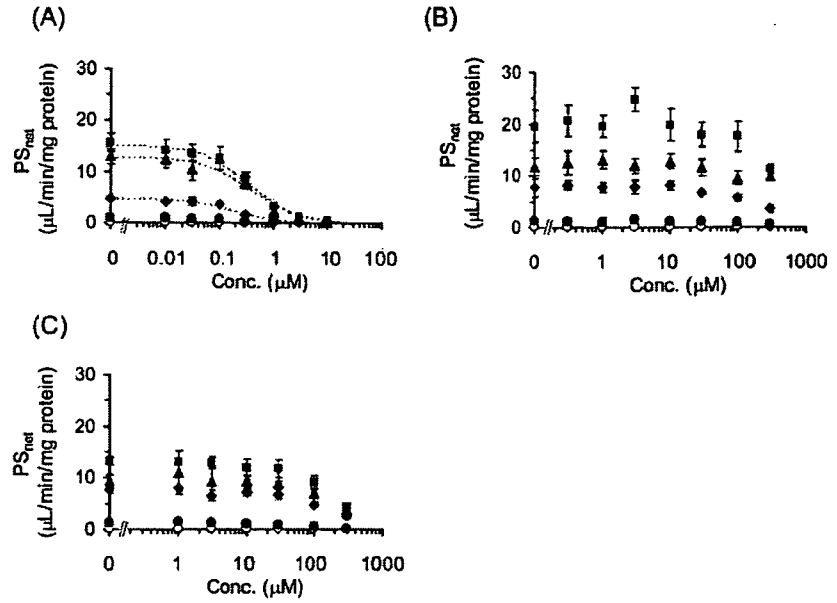

FIG. 4. Inhibitory effects of cyclosporin A, gemfibrozil, and gemfibrozil-1-*O*-glucuronide on the transcellular transport of [^{3}H]pitavastatin. The basal-to-apical flux of [^{3}H]pitavastatin (0.3 μM) across MDCKII monolayer expressing OATP1B1 (closed circles), OATP1B1/BCRP (closed diamonds), OATP1B1/MDR1 (closed squares), and OATP1B1/MRP2 (closed triangles) was determined compared with vector-transfected control cells (open circles) in the absence and presence of cyclosporin A (A), gemfibrozil (B), or gemfibrozil-1-*O*-glucuronide (C). The *x* and *y* axes represent the concentration of each inhibitor in the medium at the basal compartment and the transport clearance for the transcellular transport (PS_{net}) of [^{3}H]pitavastatin (μl/min/mg protein). Each point and vertical bar represent the mean ± S.E. of three determinations. Where vertical bars are not shown, the S.E. values are within the limits of the symbol. Dotted lines represent the fitted curves obtained by nonlinear regression analysis.

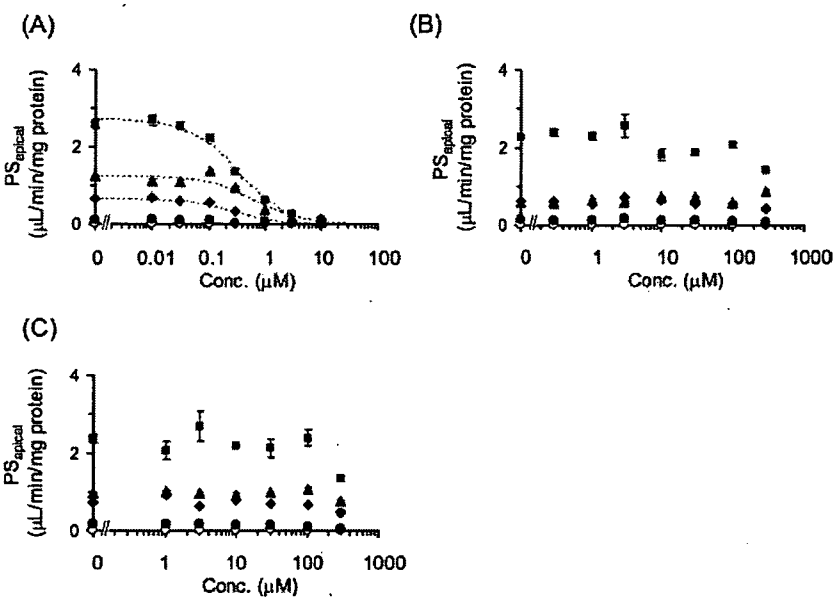

FIG. 5. Inhibitory effects of cyclosporin A, gemfibrozil, and gemfibrozil-1-*O*-glucuronide on the efflux transport of [^{3}H]pitavastatin across the apical membrane of MDCKII cells. The efflux transport clearance of [^{3}H]pitavastatin (0.3 μM) across the apical membrane (PS_{apical}) of MDCKII monolayer expressing OATP1B1 (closed circles), OATP1B1/BCRP (closed diamonds), OATP1B1/MDR1 (closed squares), and OATP1B1/MRP2 (closed triangles) was determined compared with vector-transfected control cells (open circles) in the absence and presence of cyclosporin A (A), gemfibrozil (B), or gemfibrozil-1-*O*-glucuronide (C). The *x* and *y* axes represent the concentration of each inhibitor in the medium at the basal compartment and the transport clearance for the efflux transport across the apical membrane (PS_{apical}) of [^{3}H]pitavastatin (μl/min/mg protein). Each point and vertical bar represents the mean ± S.E. of three determinations. Where vertical bars are not shown, the S.E. values are within the limits of the symbol. Dotted lines represent the fitted curves obtained by nonlinear regression analysis.

compared with pravastatin. The K_m value of E_1S for OATP2B1 from our analyses was 20.9 μM (Fig. 1), which was almost comparable to the reported values (Kullak-Ublick et al., 2001; Nozawa et al., 2004), whereas the significant uptake of $E_2 17\beta G$ at pH 7.4 was not detected as described previously (Kullak-Ublick et al., 2001; Nozawa et al., 2004).

Then, to refute the possibility that OATP2B1 plays an important role in the pitavastatin uptake in human hepatocytes and confirm the major contribution of OATP1B1, we took two strategies: 1) to check the inhibitable portion of pitavastatin uptake by two inhibitors in human hepatocytes, and 2) to compare the relative expression level of OATP2B1 in human hepatocytes and OATP2B1-expressing cells by Western blot analysis. As a result of the first approach, pitavastatin uptake in human hepatocytes was almost completely suppressed

TABLE 3

The K_i values of cyclosporin A, gemfibrozil, and gemfibrozil-1-O-glucuronide for the PS_{net} and PS_{apical} of pitavastatin in double-transfected cells

The values are expressed as mean ± computer-calculated S.D.

Transfectants	Cyclosporin A	Gemfibrozil	Gemfibrozil-1-*O*-glucuronide
PS_{net} (K_i, μM)			
OATP1B1/BCRP	0.194 ± 0.048	>100	>100
OATP1B1/MDR1	0.359 ± 0.046	>100	>100
OATP1B1/MRP2	0.407 ± 0.132	>100	>100
PS_{apical} (K_i, μM)			
OATP1B1/BCRP	0.273 ± 0.083	>300	>300
OATP1B1/MDR1	0.330 ± 0.037	>300	>300
OATP1B1/MRP2	0.662 ± 0.252	>300	>300

by both 100 μM $E_2$17βG (inhibitor of OATP1B1/OATP1B3) and E_1S (inhibitor of OATP1B1/OATP2B1) (Fig. 3), suggesting that OATP1B1 mainly contributes to the hepatic uptake of pitavastatin. In contrast, the uptake of telmisartan, which can be accepted by OATP1B3, but not OATP1B1, into human hepatocytes could not be inhibited by 100 μM E_1S (Ishiguro et al., 2006), supporting the validity of our approach. Moreover, from the comparison of the expression level of OATP2B1 between transfectants and hepatocytes by Western blot analysis (Fig. 2), we could calculate the OATP1B1-, OATP1B3-, and OATP2B1-mediated uptake into hepatocytes by multiplying the uptake clearance of pitavastatin in the expression system by the ratio of the expression level in these cells (R_{exp}). The results indicated that the contribution of OATP2B1 to the hepatic uptake of pitavastatin was less than 1%, although it is a substrate of OATP2B1, and that OATP1B1 is the most important in the hepatic uptake of pitavastatin, which is consistent with the previous results calculated from other approaches (Hirano et al., 2004).

Pitavastatin is mainly eliminated from liver in an unchanged form (Kojima et al., 2001). From the pharmacokinetic point of view, the change in the hepatic uptake clearance always directly affects the overall hepatic clearance for this type of drug (Shitara et al., 2005). Since we clarified that pitavastatin is taken up into the hepatocytes mainly by OATP1B1 in the present study, we focused on the inhibitory effects of various drugs on the OATP1B1-mediated uptake of pitavastatin. The combination therapy of statins and various drugs, such as fibrates, immune suppressants, antidiabetic drugs, antihypertensive drugs, and antibiotics, is widely used in the clinical situation (Williams and Feely, 2002). It has been reported that the plasma area under the plasma concentration-time curve of several statins was increased by coadministration of cyclosporin A and gemfibrozil (Shitara et al., 2005). Recently, Shitara et al. (2003) have demonstrated that inhibition of OATP1B1 is a major mechanism of DDI between cerivastatin and cyclosporin A. Campbell et al. (2004) also suggested that unconjugated hyperbilirubinemia induced by indinavir, rifamycin SV, and cyclosporin A is partly caused by the inhibition of OATP1B1-mediated uptake. Although pitavastatin uptake could be inhibited by several drugs in in vitro experiments, from the results of our calculation (Ito et al., 1998), the R values of most of the drugs we tested are almost equal to 1 (Table 2). To avoid the false-negative prediction of DDI, we estimated the inhibitory effects of the maximum plasma unbound concentration of inhibitors at the inlet to the liver ($I_{in,max}$). Therefore, it is unlikely that the OATP1B1-mediated DDI between pitavastatin and these drugs occurs in the clinical stage. However, we should pay attention to the OATP1B1-mediated DDI for pitavastatin with coadministration of cyclosporin A, rifampicin, rifamycin SV, clarithromycin, and indinavir because their R values exceeded 2.5 (Table 2), although the degree of the inhibition could be overestimated. We should notice that these drugs may also cause DDI with compounds that are mainly eliminated from liver via OATP1B1, including other statins. The previous clinical studies have shown that plasma concentration of pitavastatin was increased by cyclosporin A (Hasunuma et al., 2003), but not gemfibrozil and fenofibrate (Mathew et al., 2004). This evidence was consistent with our prediction (Table 2).

Conversely, gemfibrozil caused an increase in plasma concentration of cerivastatin (Backman et al., 2002). One of the major mechanisms of DDI between cerivastatin and gemfibrozil was considered to be the inhibition of CYP2C8-mediated metabolism of cerivastatin by gemfibrozil-1-*O*-glucuronide, which is thought to be concentrated in hepatocytes (Shitara et al., 2004). Gemfibrozil is metabolized into M3 and its glucuronide in the liver. Therefore, to investigate whether gemfibrozil, gemfibrozil-M3, and gemfibrozil-1-*O*-glucuronide could affect the transcellular transport by the inhibition of efflux transporter in liver, we checked their inhibitory effects on transcellular transport clearance (PS_{net}) and efflux clearance (PS_{apical}) in double-transfected cells. As a result, gemfibrozil and its metabolites could not inhibit the efflux transporters and affect transcellular transport, whereas cyclosporin A strongly inhibited both PS_{net} and PS_{apical} in all kinds of double-transfected cells (Figs. 4 and 5). This result suggested that the DDI between cyclosporin A and pitavastatin may be caused not only by the inhibition of OATP1B1-mediated uptake, but also by the inhibition of efflux transport mediated by MRP2, MDR1, and BCRP.

In conclusion, we have confirmed the major contribution of OATP1B1 to the hepatic uptake of pitavastatin in human hepatocytes. In addition, focusing on OATP1B1, inhibitory effects of various drugs on pitavastatin uptake were determined by OATP1B1-expressing cells, and its clinical relevance was discussed by considering the R values. Our results suggested that OATP1B1-mediated DDI between pitavastatin and some drugs indicated above may be clinically relevant and should be taken notice of during coadministration of inhibitors of OATP1B1.

Acknowledgments. We thank Dr. Piet Borst (The Netherlands Cancer Institutes, Amsterdam, The Netherlands) for providing the MDCKII cells expressing MRP2 and MDR1, Dr. Yoshihiro Miwa (University of Tsukuba, Japan) for providing pEB6CAGMCS/SRZeo vector, and Ying Tian and Miyuki Kambara for the construction of OATP2B1-expressing cells. We also thank Kowa Co. Ltd. (Tokyo, Japan) for providing radiolabeled pitavastatin and unlabeled pitavastatin, and Sankyo Co., Ltd. (Tokyo, Japan) and Chemtech Labo. Inc. (Tokyo, Japan) for providing gemfibrozil-1-*O*-glucuronide.

References

Aoki T, Nishimura H, Nakagawa S, Kojima J, Suzuki H, Tamaki T, Wada Y, Yokoo N, Sato F, Kimata H, et al. (1997) Pharmacological profile of a novel synthetic inhibitor of 3-hydroxy-3-methylglutaryl-coenzyme A reductase. *Arzneim-Forsch* **47**:904–909.

Backman JT, Kyrklund C, Neuvonen M, and Neuvonen PJ (2002) Gemfibrozil greatly increases plasma concentrations of cerivastatin. *Clin Pharmacol Ther* **72**:685–691.

Campbell SD, de Morais SM, and Xu JJ (2004) Inhibition of human organic anion transporting polypeptide OATP1B1 as a mechanism of drug-induced hyperbilirubinemia. *Chem-Biol Interact* **150**:179–187.

Clark WG, Brater DC, Johnson AR, and Goth A (1992) *Goth's Medical Pharmacology*, 13th ed, Mosby-Year Book, St. Louis.

Evans M and Rees A (2002) Effects of HMG-CoA reductase inhibitors on skeletal muscle: are all statins the same? *Drug Saf* **25**:649–663.

Hagenbuch B and Meier PJ (2003) The superfamily of organic anion transporting polypeptides. *Biochim Biophys Acta* **1609**:1–18.

Hardman J, Limbird L, and Gilman AG (2001) *Goodman and Gilman's The Pharmacological Basis of Therapeutics*, 9th ed, McGraw-Hill, New York.

Hasunuma T, Nakamura M, Yachi T, Arisawa N, Fukushima K, Iijima H, and Saito Y (2003) The drug-drug interactions of pitavastatin (NK-104), a novel HMG-CoA reductase inhibitor and cyclosporine. *J Clin Ther Med* **19**:381–389.

Hirano M, Maeda K, Shitara Y, and Sugiyama Y (2004) Contribution of OATP2 (OATP1B1) and OATP8 (OATP1B3) to the hepatic uptake of pitavastatin in humans. *J Pharmacol Exp Ther* **311**:139–146.

Ichimaru N, Takahara S, Kokado Y, Wang JD, Hatori M, Kameoka H, Inoue T, and Okuyama A (2001) Changes in lipid metabolism and effect of simvastatin in renal transplant recipients induced by cyclosporine or tacrolimus. *Atherosclerosis* **158**:417–423.

Ishiguro N, Maeda K, Kishimoto W, Saito A, Harada A, Ebner T, Roth W, Igarashi T, and Sugiyama Y (2006) Predominant contribution of OATP1B3 to the hepatic uptake of telmisartan, an angiotensin II receptor antagonist, in humans. *Drug Metab Dispos* **34**:1109–1115.

Ito K, Iwatsubo T, Kanamitsu S, Ueda K, Suzuki H, and Sugiyama Y (1998) Prediction of pharmacokinetic alterations caused by drug-drug interactions: metabolic interaction in the liver. *Pharmacol Rev* **50**:387–412.

Kajinami K, Takekoshi N, and Saito Y (2003) Pitavastatin: efficacy and safety profiles of a novel synthetic HMG-CoA reductase inhibitor. *Cardiovasc Drug Rev* **21**:199–215.

Kantola T, Kivisto KT, and Neuvonen PJ (1998) Erythromycin and verapamil considerably increase serum simvastatin and simvastatin acid concentrations. *Clin Pharmacol Ther* **64**:177–182.

Kimata H, Fujino H, Koide T, Yamada Y, Tsunenari Y, Yonemitsu M, and Yanagawa Y (1998) Studies on the metabolic fate of NK-104, a new inhibitor of HMG-CoA reductase: I. Absorption, distribution, metabolism and excretion in rats. *Xenobiol Metab Dispos* **13**:484–498.

Kobayashi D, Nozawa T, Imai K, Nezu J, Tsuji A, and Tamai I (2003) Involvement of human organic anion transporting polypeptide OATP-B (SLC21A9) in pH-dependent transport across intestinal apical membrane. *J Pharmacol Exp Ther* **306**:703–708.

Kojima J, Ohshima T, Yoneda M, and Sawada H (2001) Effect of biliary excretion on the pharmacokinetics of pitavastatin (NK-104) in dogs. *Xenobio Metab Dispos* **16**:497–502.

Kullak-Ublick GA, Ismair MG, Stieger B, Landmann L, Huber R, Pizzagalli F, Fattinger K, Meier PJ, and Hagenbuch B (2001) Organic anion-transporting polypeptide B (OATP-B) and its functional comparison with three other OATPs of human liver. *Gastroenterology* **120**:525–533.

Lowry OH, Rosebrough NJ, Farr AL, and Randall RJ (1951) Protein measurement with the Folin phenol reagent. *J Biol Chem* **193**:265–267

Mathew P, Cuddy T, Tracewell WG, and Salazar D (2004) An open-label study on the pharmacokinetics (PK) of pitavastatin (NK-104) when administered concomitantly with fenofibrate or gemfibrozil in healthy volunteers. *Clin Pharmacol Ther* **75**:33.

Matsushima S, Maeda K, Kondo C, Hirano M, Sasaki M, Suzuki H, and Sugiyama Y (2005) Identification of the hepatic efflux transporters of organic anions using double transfected MDCKII cells expressing human OATP1B1/MRP2, OATP1B1/MDR1 and OATP1B1/BCRP. *J Pharmacol Exp Ther* **314**:1059–1067.

Mizuno N, Niwa T, Yotsumoto Y, and Sugiyama Y (2003) Impact of drug transporter studies on drug discovery and development. *Pharmacol Rev* **55**:425–461.

Neuvonen PJ, Kantola T, and Kivisto KT (1998) Simvastatin but not pravastatin is very susceptible to interaction with the CYP3A4 inhibitor itraconazole. *Clin Pharmacol Ther* **63**:332–341.

Nozawa T, Imai K, Nezu J, Tsuji A, and Tamai I (2004) Functional characterization of pH-sensitive organic anion transporting polypeptide OATP-B in human. *J Pharmacol Exp Ther* **308**:438–445.

Olbricht C, Wanner C, Eisenhauer T, Kliem V, Doll R, Boddaert M, O'Grady P, Krekler M, Mangold B, and Christians U (1997) Accumulation of lovastatin, but not pravastatin, in the blood of cyclosporine-treated kidney graft patients after multiple doses. *Clin Pharmacol Ther* **62**:311–321.

Sasaki M, Suzuki H, Ito K, Abe T, and Sugiyama Y (2002) Transcellular transport of organic anions across a double-transfected Madin-Darby canine kidney II cell monolayer expressing both human organic anion-transporting polypeptide (OATP2/SLC21A6) and Multidrug resistance-associated protein 2 (MRP2/ABCC2). *J Biol Chem* **277**:6497–6503.

Shimizu M, Fuse K, Okudaira K, Nishigaki R, Maeda K, Kusuhara H, and Sugiyama Y (2005) Contribution of OATP (organic anion-transporting polypeptide) family transporters to the hepatic uptake of fexofenadine in humans. *Drug Metab Dispos* **33**:1477–1481.

Shitara Y, Hirano M, Sato H, and Sugiyama Y (2004) Gemfibrozil and its glucuronide inhibit the organic anion transporting polypeptide 2 (OATP2/OATP1B1:SLC21A6)-mediated hepatic uptake and CYP2C8-mediated metabolism of cerivastatin: analysis of the mechanism of the clinically relevant drug-drug interaction between cerivastatin and gemfibrozil. *J Pharmacol Exp Ther* **311**:228–236.

Shitara Y, Itoh T, Sato H, Li AP, and Sugiyama Y (2003) Inhibition of transporter-mediated hepatic uptake as a mechanism for drug-drug interaction between cerivastatin and cyclosporin A. *J Pharmacol Exp Ther* **304**:610–616.

Shitara Y, Sato H, and Sugiyama Y (2005) Evaluation of drug-drug interaction in the hepatobiliary and renal transport of drugs. *Annu Rev Pharmacol Toxicol* **45**:689–723.

Simonson SG, Raza A, Martin PD, Mitchell PD, Jarcho JA, Brown CD, Windass AS, and Schneck DW (2004) Rosuvastatin pharmacokinetics in heart transplant recipients administered an antirejection regimen including cyclosporine. *Clin Pharmacol Ther* **76**:167–177.

Sugiyama D, Kusuhara H, Shitara Y, Abe T, Meier PJ, Sekine T, Endou H, Suzuki H, and Sugiyama Y (2001) Characterization of the efflux transport of 17beta-estradiol-D-17beta-glucuronide from the brain across the blood-brain barrier. *J Pharmacol Exp Ther* **298**:316–322.

Tamai I, Nozawa T, Koshida M, Nezu J, Sai Y, and Tsuji A (2001) Functional characterization of human organic anion transporting polypeptide B (OATP-B) in comparison with liver-specific OATP-C. *Pharm Res (NY)* **18**:1262–1269.

Williams D and Feely J (2002) Pharmacokinetic-pharmacodynamic drug interactions with HMG-CoA reductase inhibitors. *Clin Pharmacokinet* **41**:343–370.

Yamaoka K, Tanigawara Y, Nakagawa T, and Uno T (1981) A pharmacokinetic analysis program (MULTI) for microcomputer. *J Pharmacobio-Dyn* **4**:879–885.

Address correspondence to: Dr. Yuichi Sugiyama, Department of Molecular Pharmacokinetics, Graduate School of Pharmaceutical Sciences, The University of Tokyo, 7-3-1 Hongo, Bunkyo-ku, Tokyo, 113-0033 Japan. E-mail: sugiyama@mol.f.u-tokyo.ac.jp

0090-9556/06/3405-743–747$20.00
DRUG METABOLISM AND DISPOSITION

DMD 34:743–747, 2006

Vol. 34, No. 5
8375/3104108
Printed in U.S.A.

INHIBITION OF OAT3-MEDIATED RENAL UPTAKE AS A MECHANISM FOR DRUG-DRUG INTERACTION BETWEEN FEXOFENADINE AND PROBENECID

Harunobu Tahara, Hiroyuki Kusuhara, Kazuya Maeda, Hermann Koepsell, Eiichi Fuse, and Yuichi Sugiyama

Graduate School of Pharmaceutical Sciences, University of Tokyo, Hongo, Bunkyo-ku, Tokyo, Japan (H.T., H.Ku., K.M., Y.S.); Pharmacokinetic Research Laboratories, Pharmaceutical Research Institute, Kyowa Hokko Kogyo Co., Ltd., Shimotogari, Nagaizumi-cho, Sunto-gun, Shizuoka, Japan (H.T., E.F.); and Institut für Anatomie und Zellbiologie, Universität Würzburg, Germany (H.Ko.)

Received November 14, 2005; accepted January 27, 2006

ABSTRACT:

Fexofenadine, a nonsedating antihistamine drug, is effective for the treatment of seasonal allergic rhinitis and chronic urticaria. Simultaneous administration of probenecid increases the plasma concentration of fexofenadine due to an inhibition of its renal elimination in healthy volunteers (*Clin Pharmacol Ther* 77:17–23, 2005). The purpose of the present study is to investigate the possibility that the drug-drug interaction between fexofenadine and probenecid involves the renal basolateral uptake process. The uptake of fexofenadine was determined in HEK293 cells expressing human organic anion transporter 1 (OAT1/*SLC22A6*), OAT2 (*SLC22A7*), OAT3 (*SLC22A8*), and organic cation transporter 2 (OCT2/*SLC22A2*). Only hOAT3-HEK showed a significantly greater accumulation of fexofenadine than that in vector-HEK, which was saturable with K_m and V_{max} values of 70.2 μM and 120 pmol/min/mg protein, respectively. Inhibition potency of probenecid for the uptake of fexofenadine was compared between hOAT3 and organic anion-transporting peptide 1B3 (hOATP1B3), a transporter responsible for the hepatic uptake of fexofenadine (*Drug Metab Dispos* 33:1477–1481, 2005). The K_i values were determined to be 1.30 and 130 μM for hOAT3 and hOATP1B3, respectively, with Hill coefficients of 0.76 and 0.64, respectively. The K_i value of probenecid for hOAT3, but not for hOATP1B3, was significantly lower than the maximum unbound plasma concentration of probenecid at clinical dosages. These results suggest that the renal drug-drug interaction between fexofenadine and probenecid is probably explained by an inhibition of the renal uptake of fexofenadine via hOAT3, at least in part.

The kidney plays important roles in the detoxification of xenobiotics and endogenous wastes as well as maintaining stable levels of electrolytes and nutrients in the body. Urinary excretion consists of glomerular filtration in the glomeruli, tubular secretion across the proximal tubules, and reabsorption. Many studies have shown the importance of transporters in the tubular secretion of a large number of organic compounds, and a number of studies have described the role of multispecific organic anion and cation transporters (OAT/*SLC22* and OCT/*SLC22*) in the renal uptake of drugs. OCT2 (*SLC22A2*) plays a predominant role in the renal uptake of organic cations in the human kidney, whereas OCT1 plays a predominant role in the hepatic uptake of organic cations in the human liver (Koepsell, 2004; Lee and Kim, 2004; Wright and Dantzler, 2004). Three isoforms of the organic anion transporter family (OAT1/*SLC22A6*, OAT2/*SLC22A7*, and OAT3/*SLC22A8*) have been identified on the basolateral membrane of the human proximal tubules (Lee and Kim, 2004; Miyazaki et al., 2004; Wright and Dantzler, 2004). It has been suggested that hOAT1 plays an important role in the renal uptake of hydrophilic organic anions with a low molecular weight, whereas hOAT3 plays an important role in the renal uptake of amphipathic organic anions as well as a basic drug, famotidine (Hasegawa et al., 2003; Tahara et al., 2005a). The mRNA of hOAT2 in the kidney is markedly lower than that of hOAT1 and hOAT3 (Motohashi et al., 2002), and its role in drug transport in the kidney remains unknown. Identification of the basolateral transporters provides a clue to understanding the molecular mechanisms of drug-drug interactions involving tubular secretion. Takeda et al. (2002) and Nozaki et al. (2004) have shown that rOat3/hOAT3-mediated renal uptake can be a potential drug-drug interaction site with some nonsteroidal anti-inflammatory drugs at clinical dosages by comparing their K_i values for rOat3/hOAT3 with the unbound plasma concentrations. In addition, we have reported that OAT3 could be the site of an interaction between famotidine and probenecid in humans (Tahara et al., 2005a).

Fexofenadine, an active metabolite of terfenadine, is a nonsedating histamine H_1 receptor antagonist that is prescribed for the oral treatment of allergic rhinitis and chronic idiopathic urticaria. After oral administration of [^{14}C]fexofenadine to healthy volunteers, 92% of the total dose was recovered, 12% in urine and 80% in feces, as the

This work was supported by Health and Labour Sciences Research Grants from the Ministry of Health, Labour and Welfare for the Research on Regulatory Science of Pharmaceuticals and Medical Devices.

Article, publication date, and citation information can be found at http://dmd.aspetjournals.org.

doi:10.1124/dmd.105.008375.

ABBREVIATIONS: OAT, organic anion transporter; hOAT, human OAT; OCT, organic cation transporter; hOCT, human OCT; r, rat; hOATP, human organic anion-transporting peptide; AUC, area under the plasma concentration-time curve; HEK, human embryonic kidney; LC-MS, liquid chromatography-mass spectrometry.

unchanged form (Lippert et al., 1995). Since the average absolute oral bioavailability of fexofenadine was reported to be 33% (Dresser et al., 2005), about 36% of the bioavailable fexofenadine can be excreted into the urine during a 24-h period, and renal elimination makes a significant contribution to the total body clearance in addition to biliary excretion. Interactions of fexofenadine with drugs and food have been reported. The interactions with rifampicin (Hamman et al., 2001), St John's wort (Wang et al., 2002), and fruit juice (Dresser et al., 2002) caused a reduction in the AUC of fexofenadine after oral administration, and these are hypothesized to include modulation of P-glycoprotein or inhibition of OATP2B1 in the small intestine (Cvetkovic et al., 1999; Nozawa et al., 2004). The interactions with verapamil (Yasui-Furukori et al., 2005) and ketoconazole (Simpson and Jarvis, 2000) increased the AUC of fexofenadine, probably because of an increase in the oral absorption produced by inhibition of intestinal P-glycoprotein. Probenecid treatment caused a significant reduction in the unbound renal clearance of fexofenadine (Yasui-Furukori et al., 2005). Because probenecid is a potent inhibitor of OATs (Tahara et al., 2005a), it is possible that this interaction involves renal transporters, such as OAT1, OAT2, and OAT3.

In the present study, to obtain an insight into the basolateral uptake mechanism of fexofenadine, the uptake was determined in cDNA-transfected cells expressing hOAT1, hOAT2, hOAT3, and hOCT2, and the effect of probenecid on the uptake was determined to examine whether it is inhibited by a clinically relevant concentration of probenecid.

Materials and Methods

Fexofenadine hydrochloride was purchased from Toronto Research Chemicals (North York, ON, Canada). Ranitidine was purchased from Sigma-Aldrich (St. Louis, MO). [^{3}H] *p*-Aminohippurate (151 GBq/mmol) was purchased from PerkinElmer Life and Analytical Sciences (Wellesley, MA). [^{3}H]Benzylpenicillin (740 GBq/mmol) was purchased from GE Healthcare UK (Little Chalfont, Buckinghamshire, UK). All other chemicals and reagents were obtained from Kanto Kagaku (Tokyo, Japan) or Wako Pure Chemicals (Osaka, Japan) and were of the highest grade available.

The stable transfectants expressing hOAT1-, hOAT2-, hOAT3- (Tahara et al., 2005a), hOCT2- (Schlatter et al., 2002), and hOATP1B3-HEK (Shimizu et al., 2005) were established as described previously. These cells were grown in Dulbecco's modified Eagle's medium (Invitrogen, Carlsbad, CA) supplemented with 10% fetal bovine serum, penicillin (100 U/ml), streptomycin (100 μg/ml), and G418 sulfate (400 μg/ml) at 37°C with 5% CO_2 and 95% humidity on the bottom of a dish. hOAT1-, hOAT2-, hOAT3-, hOCT2-, and hOATP1B3-HEK were seeded in polylysine-coated 12-well plates at a density of $1.2 \times \sim 10^5$ cells/well. The transport activity by each cell line was confirmed by examining the uptake of ranitidine by hOAT1, hOAT2, hOAT3, and hOCT2.

Transport Studies. Transport studies were carried out as described previously (Tahara et al., 2005a). Uptake was initiated by adding medium containing a 10 μM concentration of the compounds after the cells had been washed twice and preincubated with Krebs-Henseleit buffer at 37°C for 15 min. The Krebs-Henseleit buffer consisted of 142 mM NaCl, 23.8 mM $NaHCO_3$, 4.83 mM KCl, 0.96 mM KH_2PO_4, 1.20 mM $MgSO_4$, 12.5 mM HEPES, 5 mM glucose, and 1.53 mM $CaCl_2$ adjusted to pH 7.4. The uptake was terminated at a designated time by adding ice-cold Krebs-Henseleit buffer after removal of the incubation buffer. Then, cells were washed twice with 1 ml of ice-cold Krebs-Henseleit buffer. For the determination of the uptake of fexofenadine, cells were dissolved in 300 μl of 0.2 N NaOH and kept overnight. Aliquots (150 μl) were transferred to vials after adding 30 μl of 1 N HCl. Aliquots (100 μl) were used for LC-MS quantification as described below. The remaining 10 μl of the aliquots of cell lysate were used to determine the protein concentration by the method of Lowry et al. (1951) with bovine serum albumin as a standard. Ligand uptake was given as the cell-to-medium concentration ratio determined as the amount of ligand associated with cells divided by the medium concentration.

Quantification of Fexofenadine by LC-MS. A sensitive method was developed to determine fexofenadine by high-performance liquid chromatography-electrospray ionization-mass spectrometry with midazolam as the internal standard (Tahara et al., 2005b). The LC-MS consisted of an Alliance HT 2795 separation module with an autosampler (Waters, Milford, MA) and a Micromass ZQ mass spectrometer with an electro ion spray interface (Waters). The optimum operating conditions used were as follows: electrospray probe (capillary) voltage 2.7 kV, sample cone voltage 35 V, and source temperature 100°C. The spectrometer was operated at a drying desolvation gas flow rate of 300 l/h. The mass spectrometer was operated in the selected ion monitoring mode using the respective MH^+ ions, *m/z* 502.3 for fexofenadine and *m/z* 326.3 for the internal standard. The mobile phase used for high-performance liquid chromatography was: methanol (A) and 0.05% formic acid (B). Chromatographic separation was achieved on a C_{18} column (Capcell pak C_{18}, MG, 4.6 mm i.d. × 75 mm, particle size 3 μm; Shiseido, Tokyo, Japan), using a linear gradient from 55% A to 70% A over 5 min and returning to 55% A within 2 min. The quantification limit of this method was 5 nM in the cell lysate. Instrument control and data analysis were performed using MassLynx application software from Waters.

Kinetic Analyses. Kinetic parameters were obtained using the Michaelis-Menten equation: $v = V_{max} \times S/(K_m + S)$, where v is the uptake rate of the substrate (pmol/min/mg protein), S is the substrate concentration in the medium (μM), K_m is the Michaelis constant (μM), and V_{max} is the maximum uptake rate (pmol/min/mg protein). To obtain the kinetic parameters, the equation was fitted to the uptake velocity using a MULTI program (Yamaoka et al., 1981). The input data were weighted as the reciprocals of the squares of the observed values. Inhibition constants (K_i) of several compounds were calculated assuming competitive inhibition using the following equation: $CL_{+inh} = CL/(1 + (I/K_i)^S)$, where CL is the uptake clearance, I is the concentration of inhibitor (μM), and S is the Hill coefficient. The subscript (+inh) represents the value in the presence of inhibitor. The substrate concentration was low compared with its K_m value in the inhibition study. The two-tailed unpaired *t* test was used for a statistical analysis and a value of p less than 0.05 was considered significant.

Results

Time Profile of the Uptake of Fexofenadine by hOAT1-, hOAT2-, hOAT3-, and hOCT2-HEK. Figure 1 shows the time profiles of the uptake of the typical substrates and fexofenadine by hOAT1-, hOAT2-, hOAT3-, hOCT2-, and vector-HEK cells. Consistent with our previous report (Tahara et al., 2005a,c), the uptake of the typical substrates by the cDNA transfectants was significantly greater than that in vector-HEK. The uptake of fexofenadine by hOAT3-HEK was significantly greater than that in vector-HEK at all time points, whereas the uptake by hOAT1-, hOAT2-, and hOCT2-HEK was very similar to that of vector-HEK (Fig. 1). Since the uptake of fexofenadine by hOAT3-HEK increased linearly up to 5 min of incubation, the uptake of fexofenadine for 5 min was used for further characterization.

Concentration Dependence of the Uptake of Fexofenadine by hOAT3-HEK, and the Effect of Probenecid. The concentration dependence of the uptake of fexofenadine by hOAT3-HEK was examined (Fig. 2). The uptake was saturable, and the K_m and V_{max} values, determined by nonlinear regression analysis, were 70.2 ± 2.7 μM and 120 ± 3 pmol/min/mg protein, respectively. The inhibitory effect of probenecid on hOAT3-mediated uptake of fexofenadine was examined (Fig. 3). The K_i value of probenecid for the uptake of fexofenadine by hOAT3-HEK was determined to be 1.30 ± 0.30 μM with a Hill coefficient of 0.76.

Time Profile of the Uptake of Fexofenadine by hOATP1B3-HEK, and the Effect of Probenecid. As reported previously by Shimizu et al. (2005), the uptake of fexofenadine using the same hOATP1B3-HEK was greater than that by mock cells (7.59 ± 0.26 versus 3.97 ± 0.22 μl/mg protein at 5 min) (Fig. 4A). The K_i value of probenecid for the uptake of fexofenadine by hOATP1B3-HEK was determined to be 130 ± 40 μM with a Hill coefficient of 0.64 (Fig.

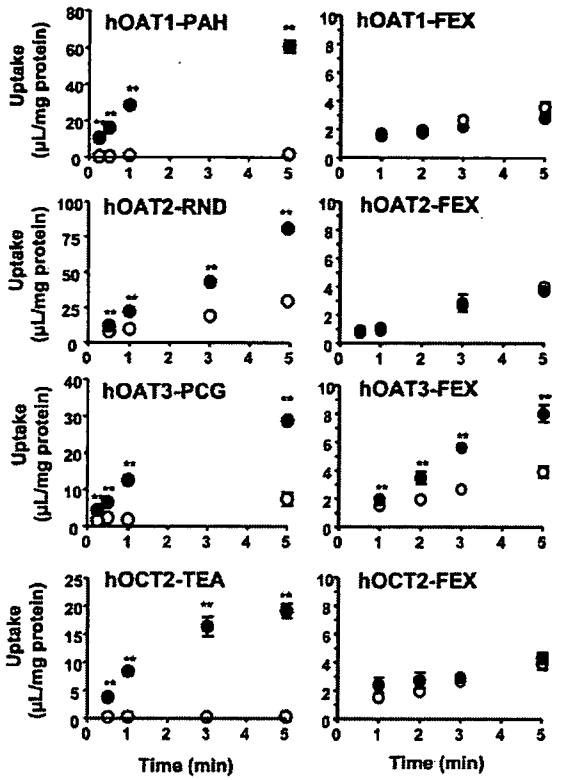

FIG. 1. Time profile of the uptake of typical substrates and fexofenadine by hOAT1-, hOAT2-, hOAT3-, and hOCT2-HEK. The time-dependent uptake of the typical substrates and fexofenadine (10 μM) by hOAT1-, hOAT2-, hOAT3-, and hOCT2-HEK was examined at 37°C. Closed and open circles represent the uptake by OATs/OCTs-HEK and vector-HEK, respectively. Statistical differences in the uptake of OATs/OCTs-HEK were compared with vector-HEK by a two-tailed unpaired t test with $p < 0.05$ as the limit of significance (*, $p < 0.05$; **, $p < 0.01$). Each point represents the mean ± S.E. (n = 3). PAH, p-aminohippurate; RND, ranitidine; PCG, benzylpenicillin; TEA, tetraethylammonium; FEX, fexofenadine.

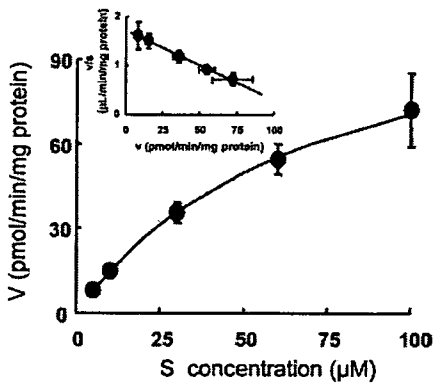

FIG. 2. Concentration dependence of the uptake of fexofenadine by hOAT3-HEK. The hOAT3-mediated uptake of fexofenadine for 5 min was determined at various concentrations (5–100 μM, range of concentrations used). The hOAT3-mediated transport was obtained by subtracting the transport velocity in vector-HEK from that in rOat3-HEK. In the inset, the concentration dependence of hOAT3-mediated fexofenadine uptake is shown as an Eadie-Hofstee plot. Each point represents the mean ± S.E. (n = 3). Where bars are not shown, the S.E. is contained within the limits of the symbol.

4B). Probenecid is a 100-fold more potent inhibitor of hOAT3 than hOATP1B3.

Discussion

Fexofenadine is an orally active nonsedative histamine H1 receptor antagonist. Only a small amount of the orally administered [^{14}C]fexofenadine was recovered in the urine of healthy volunteers (12%), and urinary excretion has been considered to be a minor elimination pathway. However, the fact that the absolute oral bioavailability of fexofenadine is, on average, 33% means that a considerable amount of fexofenadine is excreted into the urine over a 24-h period (36% of the amount absorbed into the circulating blood) and suggests that renal elimination makes a significant contribution to the total clearance. The renal clearance of fexofenadine is greater than the glomerular filtration rate, indicating that tubular secretion accounts for the major part of the renal clearance (Table 1). Simultaneously administered probenecid caused an approximately 50% increase in the AUC of fexofenadine in healthy subjects, and this is largely explained by a 73% inhibition of the renal clearance of fexofenadine (Table 1) (Yasui-Furukori et al., 2005). In the present study, we examined the possible role of renal organic anion and cation transporters in the drug-drug interaction between fexofenadine and probenecid.

In cDNA-transfected cells, fexofenadine is efficiently transported only by hOAT3, whereas specific uptake by hOAT1, hOAT2, and hOCT2 was below the limit of detection, suggesting that hOAT3 plays a major role in the renal uptake of fexofenadine (Fig. 1). The transport activity of fexofenadine by hOAT3 was much lower than that of benzylpenicillin (1.71 versus 10.7 μl/min/mg protein). This was in good agreement with clinical data showing that the renal tubular secretion clearance of benzylpenicillin in healthy volunteers was 983 ml/min (Bins and Mattie, 1988), at least 9-fold higher than that of fexofenadine (113 ml/min, Table 1). Probenecid is a potent inhibitor

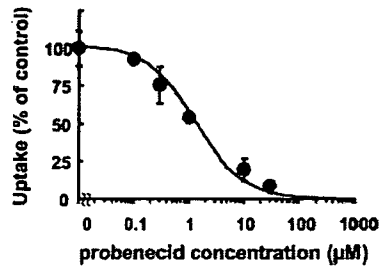

FIG. 3. Inhibitory effect of probenecid on the uptake of fexofenadine by hOAT3-HEK. The uptake of fexofenadine (10 μM) by hOAT3- and hOATP1B3-HEK for 5 min was determined in the absence or presence of probenecid at the designated concentrations. The values are expressed as a percentage of fexofenadine transport by hOAT3- or hOATP1B3-HEK in the presence of inhibitors versus that in the absence of inhibitors. The Hill coefficient value was 0.763 ± 0.047. Each point represents the mean ± S.E. (n = 3).

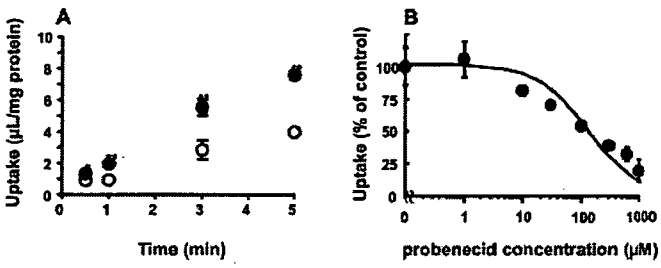

FIG. 4. Time profile of the uptake of fexofenadine by hOATP1B3 and the inhibitory effect of probenecid on the uptake of fexofenadine by hOATP1B3-HEK. The time-dependent uptake of fexofenadine (10 μM) by hOATP1B3-HEK was examined at 37°C. Closed and open circles represent the uptake by hOATO1B3-HEK and vector-HEK, respectively (A). The uptake of fexofenadine (10 μM) by hOATP1B3-HEK for 5 min was determined in the absence or presence of probenecid at the designated concentrations (B). The values are expressed as a percentage of fexofenadine transport by hOATP1B3-HEK in the presence of inhibitors versus that in the absence of inhibitors. The Hill coefficient value was 0.642 ± 0.079. Statistical differences in the uptake of hOATP1B3-HEK were compared with that by vector-HEK using a two-tailed unpaired t test with $p < 0.05$ as the limit of significance (*, $p < 0.05$; **, $p < 0.01$). Each point represents the mean ± S.E. (n = 3).

TABLE 1

Effects of cimetidine and probenecid treatments on pharmacokinetic parameters of fexofenadine

Parameter	Control	Cimetidine	Probenecid
$AUC_{(0-\infty)}$ (ng · h/ml)	3637 ± 1199	4124 ± 2019	6150 ± 3972
Ratio to control	1	1.08	1.53
$CL_{renal,\ u}$ (ml/min)[a]	230 ± 78	152 ± 70	74 ± 52
Ratio to control	1	0.610	0.270
CL_{sc} (ml/min)[b]	133	55.0	0 (almost)
Ratio to control	1	0.414	0 (almost)
$I_{u,\ max}$[c]		5.20	24.0
K_i (K_m) for hOAT3		(113)	1.30
R[d]		0.956	0.0514

[a] $CL_{renal,\ u}$, unbound renal clearance (Yasui-Furukori et al., 2005).
[b] CL_{sc}, tubular secretion clearance ($CL_{renal,\ u} - CL_{creatinine}$). Creatinine clearance value was used for the value of glomerular filtration rate (97 ml/min; van Crugten et al., 1985).
[c] $I_{u,\ max}$, maximum unbound plasma concentration of inhibitor (Selen et al., 1982; van Crugten et al., 1985).
[d] R value was calculated according to the following equation: $R = 1/(1 + I_{u,\ max}/K_i)$.

of hOAT3, and the unbound plasma concentration of probenecid at clinical doses (0.5–2.0 g), ranging from 12 to 52 μM (Selen et al., 1982), is greater than its K_i value for hOAT3 (Table 1; Fig. 3). Therefore, probenecid will produce almost complete inhibition of hOAT3 in clinical situations, consistent with clinical reports, 73% inhibition of the renal clearance of fexofenadine by probenecid (Yasui-Furukori et al., 2005). Therefore, inhibition of basolateral uptake can be one of the sites of interaction between fexofenadine and probenecid. Cimetidine inhibits the renal clearance of fexofenadine by 39% on average in healthy subjects (Table 1). Since the clinical plasma concentration of unbound cimetidine at a dose of 400 mg was reported to be 5.2 μM (van Crugten et al., 1986), far below its K_m and IC_{50} values for hOAT3 [113 μM (Tahara et al., 2005c) and 92.4 μM (Khamdang et al., 2004), respectively], it is unlikely that the interaction involves hOAT3. Cimetidine may inhibit efflux process across the brush-border membrane of the proximal tubules. Although fexofenadine has been shown to be a substrate of P-glycoprotein (Cvetkovic et al., 1999; Tahara et al., 2005b), the steady-state plasma concentration was unchanged in Mdr1a/1b knockout mice (Tahara et al., 2005b), suggesting its limited role in the urinary and biliary excretion, and the transporter responsible for the luminal efflux remains unknown. Further studies are necessary to investigate whether the transporter responsible for the luminal efflux is another site of drug-drug interaction with probenecid and cimetidine.

The nonrenal clearance of fexofenadine is explained by biliary excretion. It was found that fexofenadine is a substrate of hOATP1B3, whereas the specific uptake of fexofenadine by OATP1B1 and OATP2B1 is very low (Shimizu et al., 2005). Based on quantitative prediction using the concept of a relative activity factor, hOATP1B3 has been suggested to play a major role in the hepatic uptake of fexofenadine (Shimizu et al., 2005). Our inhibition study revealed that probenecid is a weak inhibitor of hOATP1B3, with a K_i value greater than the unbound concentration achieved by a clinical dose (1 g) of probenecid (24 μM; Selen et al., 1982). Therefore, probenecid probably exhibits only a minimal inhibitory effect on the hepatic uptake of fexofenadine via hOATP1B3. This is consistent with the kinetic consideration that the drug-drug interaction is largely explained by a 73% inhibition of the renal clearance of fexofenadine.

The effect of probenecid on the total body clearance will be less potent in rats because of the smaller contribution of the renal clearance of fexofenadine to the total clearance (15–20%) (Kamath et al., 2005). There are two possibilities to account for this. One is the species difference in OAT3-mediated transport, i.e., basolateral uptake process since OAT3-mediated transport shows poor correlation between rat and human (Tahara at al., 2005c). The other is reabsorption mediated by Oatp1a1 in rats. Oatp1a1 is localized on the brush-border membrane of the kidney (Bergwerk et al., 1996), whereas its human homolog, OATP1A2, exhibits brain-specific distribution (Abe et al., 1999). Oatp1a1 has been suggested to be involved in the reabsorption of amphipathic organic anions (Gotoh et al., 2002). Since fexofenadine is a substrate of Oatp1a1 (Cvetkovic et al., 1999), it is likely that it undergoes reabsorption from the lumen by Oatp1a1 in the rat kidney. Oatp1a1 expression exhibits gender difference, leading to the gender difference in the renal clearance of amphipathic organic anions (Gotoh et al., 2002). Female rats may be a better animal model to investigate the pharmacokinetics in humans.

The present study highlights the underlying mechanism of the drug-drug interaction with probenecid focusing on OAT3. Probenecid is also a potent inhibitor of OAT1, and its K_i value is smaller than the clinical unbound plasma concentration of probenecid. Therefore, both OAT1 and OAT3 can be a site of drug-drug interaction with probenecid. This is why probenecid causes a drug-drug interaction with a number of drugs in terms of renal elimination (Cunningham et al., 1981). Adefovir and cidofovir have been suggested to be taken up by the kidney via human OAT1(Ho et al., 2000; Mulato et al., 2000). They are nucleoside phosphonate analogs, a class of novel antivirals structurally related to natural nucleotides, and nephrotoxicity is their main dose-limiting toxic effect. Ho et al. (2000) and Mulato et al. (2000) have demonstrated that hOAT1 is directly involved in the induction of nephrotoxicity since the expression of hOAT1 sensitized a mammary cell line to adefovir and cidofovir, and probenecid reduced the cytotoxicity (Ho et al., 2000; Mulato et al., 2000). In such circumstances, combination with probenecid will have a beneficial effect in suppressing the nephrotoxicity as well as prolonging their plasma retention time, leading to an increase in the concentration in the liver, the target organ for the treatment of hepatitis B.

In conclusion, hOAT3 shows specific uptake of fexofenadine among basolateral transporters and accounts for its renal uptake. Probenecid is a potent inhibitor of hOAT3, and inhibition of hOAT3 is a likely mechanism to account for the increase in the AUC of fexofenadine caused by probenecid treatment in healthy subjects.

References

Abe T, Kakyo M, Tokui T, Nakagomi R, Nishio T, Nakai D, Nomura H, Unno M, Suzuki M, Naitoh T, et al. (1999) Identification of a novel gene family encoding human liver-specific organic anion transporter LST-1. *J Biol Chem* **274**:17159–17163.

Bergwerk AJ, Shi X, Ford AC, Kanai N, Jacquemin E, Burk RD, Bai S, Novikoff PM, Stieger B, Meier PJ, et al. (1996) Immunologic distribution of an organic anion transport protein in rat liver and kidney. *Am J Physiol* **271**:G231–G238.

Bins JW and Mattie H (1988) Saturation of the tubular excretion of beta-lactam antibiotics. *Br J Clin Pharmacol* **25**:41–50.

Cunningham RF, Israili ZH, and Dayton PG (1981) Clinical pharmacokinetics of probenecid. *Clin Pharmacokinet* **6**:135–151.

Cvetkovic M, Leake B, Fromm MF, Wilkinson GR, and Kim RB (1999) OATP and P-glycoprotein transporters mediate the cellular uptake and excretion of fexofenadine. *Drug Metab Dispos* **27**:866–871.

Dresser GK, Bailey DG, Leake BF, Schwarz UI, Dawson PA, Freeman DJ, and Kim RB (2002) Fruit juices inhibit organic anion transporting polypeptide-mediated drug uptake to decrease the oral availability of fexofenadine. *Clin Pharmacol Ther* **71**:11–20.

Dresser GK, Kim RB, and Bailey DG (2005) Effect of grapefruit juice volume on the reduction of fexofenadine bioavailability: possible role of organic anion transporting polypeptides. *Clin Pharmacol Ther* **77**:170–177.

Gotoh Y, Kato Y, Stieger B, Meier PJ, and Sugiyama Y (2002) Gender difference in the Oatp1-mediated tubular reabsorption of estradiol 17beta-D-glucuronide in rats. *Am J Physiol* **282**:E1245–E1254.

Hamman MA, Bruce MA, Haehner-Daniels BD, and Hall SD (2001) The effect of rifampin administration on the disposition of fexofenadine. *Clin Pharmacol Ther* **69**:114–121.

Hasegawa M, Kusuhara H, Endou H, and Sugiyama Y (2003) Contribution of organic anion transporters to the renal uptake of anionic compounds and nucleoside derivatives in rat. *J Pharmacol Exp Ther* **305**:1087–1097.

Ho ES, Lin DC, Mendel DB, and Cihlar T (2000) Cytotoxicity of antiviral nucleotides adefovir and cidofovir is induced by the expression of human renal organic anion transporter 1. *J Am Soc Nephrol* **11**:383–393.

Kamath AV, Yao M, Zhang Y, and Chong S (2005) Effect of fruit juices on the oral bioavailability of fexofenadine in rats. *J Pharm Sci* **94**:233–239.

Khamdang S, Takeda M, Shimoda M, Noshiro R, Narikawa S, Huang XL, Enomoto A, Piyachaturawat P, and Endou H (2004) Interactions of human- and rat-organic anion transporters with pravastatin and cimetidine. *J Pharmacol Sci* **94**:197–202.

Koepsell H (2004) Polyspecific organic cation transporters: their functions and interactions with drugs. *Trends Pharmacol Sci* **25**:375–381.
Lee W and Kim RB (2004) Transporters and renal drug elimination. *Annu Rev Pharmacol Toxicol* **44**:137–166.
Lippert C, Ling J, Brown P, Burmaster S, Eller M, Cheng L, Thompson R, and Weir S (1995) Mass balance and pharmacokinetics of MDL 16455A in healthy male volunteers. *Pharm Res (NY)* **12**:S390.
Lowry OH, Rosebrough NJ, Farr AL, and Randall RJ (1951) Protein measurement with the Folin phenol reagent. *J Biol Chem* **193**:265–267.
Miyazaki H, Sekine T, and Endou H (2004) The multispecific organic anion transporter family: properties and pharmacological significance. *Trends Pharmacol Sci* **25**:654–662.
Motohashi H, Sakurai Y, Saito H, Masuda S, Urakami Y, Goto M, Fukatsu A, Ogawa O, and Inui K (2002) Gene expression levels and immunolocalization of organic ion transporters in the human kidney. *J Am Soc Nephrol* **13**:866–874.
Mulato AS, Ho ES, and Cihlar T (2000) Nonsteroidal anti-inflammatory drugs efficiently reduce the transport and cytotoxicity of adefovir mediated by the human renal organic anion transporter 1. *J Pharmacol Exp Ther* **295**:10–15.
Nozaki Y, Kusuhara H, Endou H, and Sugiyama Y (2004) Quantitative evaluation of the drug-drug interactions between methotrexate and nonsteroidal anti-inflammatory drugs in the renal uptake process based on the contribution of organic anion transporters and reduced folate carrier. *J Pharmacol Exp Ther* **309**:226–234.
Nozawa T, Imai K, Nezu J, Tsuji A, and Tamai I (2004) Functional characterization of pH-sensitive organic anion transporting polypeptide OATP-B. *J Pharmacol Exp Ther* **308**: 438–445.
Schlatter E, Monnich V, Cetinkaya I, Mehrens T, Ciarimboli G, Hirsch JR, Popp C, and Koepsell H (2002) The organic cation transporters rOCT1 and hOCT2 are inhibited by cGMP. *J Membr Biol* **189**:237–244.
Selen A, Amidon GL, and Welling PG (1982) Pharmacokinetics of probenecid following oral doses to human volunteers. *J Pharm Sci* **71**:1238–1242.
Shimizu M, Fuse K, Okudaira K, Nishigaki R, Maeda K, Kusuhara H, and Sugiyama Y (2005) Contribution of OATP family transporters to the hepatic uptake of fexofenadine in humans. *Drug Metab Dispos* **33**:1477–1481.
Simpson K and Jarvis B (2000) Fexofenadine: a review of its use in the management of seasonal allergic rhinitis and chronic idiopathic urticaria. *Drugs* **59**:301–321.
Tahara H, Kusuhara H, Endou H, Koepsell H, Imaoka T, Fuse E, and Sugiyama Y (2005a) A species difference in the transport activities of H_2 receptor antagonists by rat and human renal organic anion and cation transporters. *J Pharmacol Exp Ther* **315**:337–345.
Tahara H, Kusuhara H, Fuse E, and Sugiyama Y (2005b) P-glycoprotein plays a major role in the efflux of fexofenadine in the small intestine and blood-brain barrier, but only a limited role in its biliary excretion. *Drug Metab Dispos* **33**:963–968.
Tahara H, Shono M, Kusuhara H, Kinoshita H, Fuse E, Takadate A, Otagiri M, and Sugiyama Y (2005c) Molecular cloning and functional analyses of OAT1 and OAT3 from cynomolgus monkey kidney. *Pharm Res (NY)* **22**:647–660.
Takeda M, Khamdang S, Narikawa S, Kimura H, Hosoyamada M, Cha SH, Sekine T, and Endou H (2002) Characterization of methotrexate transport and its drug interactions with human organic anion transporters. *J Pharmacol Exp Ther* **302**:666–671.
van Crugten J, Bochner F, Keal J, and Somogyi A (1986) Selectivity of the cimetidine-induced alterations in the renal handling of organic substrates in humans. Studies with anionic, cationic and zwitterionic drugs. *J Pharmacol Exp Ther* **236**:481–487.
Wang Z, Hamman MA, Huang SM, Lesko LJ, and Hall SD (2002) Effect of St John's wort on the pharmacokinetics of fexofenadine. *Clin Pharmacol Ther* **71**:414–420.
Wright SH and Dantzler WH (2004) Molecular and cellular physiology of renal organic cation and anion transport. *Physiol Rev* **84**:987–1049.
Yamaoka K, Tanigawara Y, Nakagawa T, and Uno T (1981) A pharmacokinetic analysis program (MULTI) for microcomputer. *J Pharmacobio-Dyn* **4**:879–885.
Yasui-Furukori N, Uno T, Sugawara K, and Tateishi T (2005) Different effects of three transporting inhibitors, verapamil, cimetidine and probenecid, on fexofenadine pharmacokinetics. *Clin Pharmacol Ther* **77**:17–23.

Address correspondence to: Dr. Yuichi Sugiyama, Professor, Graduate School of Pharmaceutical Sciences University of Tokyo Hongo, Bunkyo-ku, Tokyo, 113-0033, Japan. E-mail: sugiyama@mol.f.u-tokyo.ac.jp

Journal of Clinical Pharmacy and Therapeutics (2007) 32, 177–185

ORIGINAL ARTICLE

Adverse events caused by drug interactions involving glucuronoconjugates of zidovudine, valproic acid and lamotrigine, and analysis of how such potential events are discussed in package inserts of Japan, UK and USA

M. Hirata-Koizumi PhD, M. Saito MSc, S. Miyake PhD and R. Hasegawa PhD
Division of Medicinal Safety Science, National Institute of Health Sciences, Setagaya-ku, Tokyo, Japan

SUMMARY

Background and objective: As pharmacokinetic drug interactions frequently cause adverse events, it is important that the relevant information is given in package inserts (PIs). We previously analysed the provision of PIs for HMG-CoA reductase inhibitors and Ca antagonists, for which metabolism by cytochrome P450 could be a major interaction mechanism. In this article, we focus on interactions involving glucuronoconjugates because many drugs and their metabolites undergo this conjugation.

Methods: We reviewed clinical drug interactions related to glucuronoconjugates, focusing on reports of adverse events. Then, we picked out three important drugs (zidovudine, valproic acid and lamotrigine), and examined how the literature information is reflected in the relevant PIs in Japan, UK and USA.

Results and discussion: Pharmacokinetic interactions related to glucuronoconjugates were found with 33 drug combinations. Of these, five combinations induced clear adverse events: (i) severe anaemia due to zidovudine and caused by interaction with valproic acid, (ii) recurrence/increased frequency of seizure or increased manic states from a reduction in therapeutic effects of valproic acid caused by panipenem, (iii) meropenem or (iv) ritonavir and (v) of lamotrigine caused by oral contraceptives. Analysis of PIs showed a lack of description of the interaction of zidovudine with valproic acid in the Japanese PI. The UK PI mentioned this interaction without quantitative data, whereas full information was given in the US PI. A lack of description was also present on the interaction between valproic acid with ritonavir, reported in 2006, in the PIs of all three countries. For the interactions involving valproic acid and panipenem or meropenem, even though marked reduction of blood valproic acid level has been reported, no quantitative data were provided in any of the PIs.

Conclusion: Five combinations were identified to cause severe adverse events because of interactions related to glucuronoconjugates. This information, including quantitative data, is not always properly provided in the relevant PIs in Japan, UK or USA. PIs should be improved to better inform healthcare providers and thereby help them and their patients.

Keywords: adverse event, drug interaction, glucuronidation, glucuronoconjugate, package insert

Received 16 January 2006, Accepted 30 January 2007
Correspondence: M. Hirata-Koizumi, Division of Medicinal Safety Science, National Institute of Health Sciences, 1-18-1 Kamiyoga, Setagaya-ku, Tokyo 158-8501, Japan. Tel.: +81 3 37009528; fax: +81 3 37009788; e-mail: mkoizumi@nihs.go.jp

INTRODUCTION

Drugs are frequently co-administered with other drugs, which can change their pharmacokinetics (PK) as reflected by parameters such as area under the blood concentration time curve (AUC), maximum blood concentration (C_{max}) and half-life ($t_{1/2}$). Since such PK changes due to interactions may cause adverse effects, it is important to provide appropriate information in package inserts (PIs). We previously reported on the provision of PK interaction information in PIs of HMG-CoA reductase inhibitors and Ca antagonists (1, 2). For these two groups of drugs, the major interaction

mostly involved metabolism by cytochrome P450. Drug transporters are implicated in some cases. In this article, we focus on glucuronidation because many drugs and their metabolites undergo this conjugation (3).

In the glucuronidation reaction, catalysed by UDP-glucuronosyltransferase (UGT), glucuronic acid is transferred from UDP-glucuronic acid to the drug molecule to make it more hydrophilic and thus more easily excreted (4). Various *in vitro* studies indicate potential drug interactions via glucuronidation (5). However, two recent reviews (5, 6), focusing on PK changes resulting from the interactions, showed that reported changes in the AUC of target drugs are typically less than 2-fold in co-medication with the effective drugs. Although these small changes may be clinically meaningless in most cases, it is necessary to provide appropriate information in PIs when adverse events are found or predictable. Therefore, we reviewed clinically important glucuronidation-related PK interactions, focusing on reports of adverse events, and then analysed how the relevant information is reflected in the Japanese, UK and US PIs for three important drugs.

METHODS

We conducted a MEDLINE search for keywords, 'glucuron*' and 'interact*', from 1966 to June 2006, and then extracted clinical glucuronidation-related drug interactions with changes in AUC, C_{max}, $t_{1/2}$ or blood concentration of the parent drugs. As the mechanism of interactions is not always mentioned clearly, we directed this study to drug interactions, which were considered to occur through the formation or elimination of glucuronoconjugates. Then, we collected and reviewed adverse event data for all extracted combinations. Finally, we examined how this important literature information is reflected in the Japanese, EU and US PIs, focusing on three important drugs (zidovudine, valproic acid and lamotrigine). The current Japanese PIs were obtained from the website of the Pharmaceuticals and Medical Device Agency (http://www.pmda.go.jp). As there is no centralized authorization of these drugs in the EU, we obtained UK PIs from the electronic Medicines Compendium website (http://emc.medicines.org.uk), and analysed them. The US PIs were obtained using the Physicians' Desk Reference Electronic Library, version 7.0.306a – 2006.1 (7). Each web site was accessed from February to August 2006.

RESULTS

Literature information on drug interactions related to glucuronoconjugates

Table 1 shows 33 drug combinations for which a clinical PK glucuronidation interaction has been reported, with a summary of relevant literature information (change ratio of AUC, C_{max}, $t_{1/2}$ or blood concentration of parent drugs and adverse events or changes in pharmacological action). Although most increases in PK parameters or blood concentrations were less than 2-fold, marked decreases were also reported. Seven combinations, described below, led to adverse events or changes in pharmacological action.

In an HIV-infected patient undergoing treatment with antiretroviral regimens including zidovudine (600 mg/day), severe anaemia (haemoglobin level: 22 g/L) was recognized approximately 2 months after starting co-administration of valproic acid (1000 mg/day) (haemoglobin level measured 126 g/L at onset of the co-medication) (9). Although there was no data on the blood level of zidovudine in this case, a crossover study using 6 HIV-seropositive patients showed a 1·8-fold increase in zidovudine AUC after valproic acid co-administration for 4 days (zidovudine; 300 mg/day, valproic acid; 750 or 1500 mg/day) without changes in haematological parameters (8). It was reported that approximately 75% of oral zidovudine dose was excreted as the glucuronoconjugate in urine in humans (55). In an *in vitro* study using human liver microsomes, valproic acid inhibited UGT activity toward zidovudine within the clinical concentration range (56), thereby providing a possible mechanism for the interaction.

There were nearly 20 case reports of epilepsy patients showing a marked decrease in blood concentration of valproic acid (to <10% at maximum) with concomitant administration of panipenem or meropenem (18–25). Seven of the cases resulted in recurrence or increased frequency of seizure 2–16 days after starting the co-medication. The major pathway for metabolism of valproic acid

Table 1. Literature information on clinically relevant drug-interactions involving glucuronoconjugates

Affected drugs	Effectors	PK change[a] AUC	C_{max}	$t_{1/2}$	Adverse events or changes in pharmacological action	References
Zidovudine	Valproic acid	1·8	1·4	1·1	severe anaemia[b]	(8, 9)
	Fluconazole	1·1–1·8	1·0–1·8	1·1–2·3	–	(10, 11)
	Probenecid	1·6–2·1	1·4	1·4	–	(12, 13)
	Methadone	1·2–1·4	1·1–1·3	1·0–1·2	–	(14)
	Atovaquone	1·3	1·0	1·0	–	(15)
	Rifampicin	0·5	0·5	0·9	–	(16)
	Ritonavir	0·7	0·7	1·0	–	(17)
Valproic acid	Panipenem	<0·1–0·4[b,c]			increased frequency of seizure[b]	(18, 19)
	Meropenem	<0·1–0·5[b,c]			recurrence/increased frequency of seizure[b]	(20–25)
	Imipenem	0·5[b,c]			–[b]	(20, 21)
	Ritonavir[d]	0·5[b,c]			increased manic states[b]	(26)
Lamotrigine	Oral contraceptives	0·5	0·6	n.d.	recurrence/increased frequency of seizure[b]	(27, 28)
	Rifampicin	0·6	1·0	0·6	–	(29)
	Ritonavir[e]	0·5	0·6	0·5	–	(30)
Lorazepam	Probenecid	n.d.	n.d.	2·3	–	(31)
Temazepam	Oral contraceptives	0·6	0·8	0·6	less sedative	(32, 33)
Olanzapine	Probenecid	1·3	1·2	n.d.	–	(34)
Indomethacin	Probenecid	1·7	n.d.	1·1	increased antirheumatic effects	(35)
Acetaminophen	Probenecid	1·1	1·3	1·6–1·7	–	(31, 36)
	Propranolol	n.d.	1·5	1·3	–	(37)
	Ranitidine	1·6	1·9	n.d.	–	(38)
	Oral contraceptives	n.d.	1·1	0·7–0·9	–	(39–41)
Isofezolac	Probenecid	1·7–2·2	1·4–1·7	n.d.	–	(42)
Ketoprofen	Probenecid	2·3	1·6–1·7	1·9	–	(43, 44)
Naproxen	Probenecid	1·8–2·5	1·0–1·3	1·4–2·6	–	(45)
Zomepirac	Probenecid	4·3	2·2	n.d.	–	(46)
Diflunisal	Probenecid	1·5–1·7[c]			–	(47, 48)
Mycophenolate mofetil	Tacrolimus	1·6[f,g]	1·3[f,g]	n.d.	–	(49)
	Rifampicin	0·3[b,f]	0·5[b,f]	n.d.	–[b]	(50)
Phenprocoumon	Oral contraceptives	0·8	1·0	0·9	–	(51)
Clofibrate	Probenecid	1·8[d]			–	(52)
	Oral contraceptives	n.d.	n.d.	0·6	–	(53)
Ethinyl oestradiol	Ritonavir	0·6	0·7	0·8	–	(54)

[a]Change ratio of AUC, C_{max}, $t_{1/2}$ or blood concentration of parent drugs in co-administration to control value.
[b]Case report.
[c]Blood concentration.
[d]The interaction was reported after starting antiretroviral treatment of lopinavir/ritonavir, zidovudine and lamivudine. The authors (26) suggested ritonavir was the most likely causative agent.
[e]The interaction was reported in combination of lamotrigine and lopinavir/ritonavir in clinical study. The authors (30) suggested ritonavir was the most likely causative agent.
[f]Plasma level of mycophenolic acid (active form of mycophenolate mofetil).
[g]Results of non-crossover study with renal transplant patients, and those receiving mycophenolate mofetil with cyclosporine were selected as a control.
–, Not reported; n.d., no data available.

